Measurements of N_2O isotopologues in the stratosphere: Influence of transport on the apparent enrichment factors and the isotopologue fluxes to the troposphere

Sunyoung Park
Department of Earth and Planetary Science, University of California, Berkeley, California, USA

Elliot L. Atlas
Atmospheric Chemistry Division, National Center for Atmospheric Research, Boulder, Colorado, USA

Kristie A. Boering
Department of Earth and Planetary Science, University of California, Berkeley, California, USA

Department of Chemistry, University of California, Berkeley, California, USA

Earth Science Division, Lawrence Berkeley National Laboratory, Livermore, California, USA

Received 28 April 2003; revised 3 October 2003; accepted 10 October 2003; published 15 January 2004.

[1] Stratospheric N_2O is known to be enriched in the heavy isotopes ^{15}N and ^{18}O relative to tropospheric N_2O, primarily because of the preferential photolysis of light isotopologues. We present measurements of $\delta^{15}N$, $\delta^{18}O$, and site-specific $\delta^{15}N$ on N_2O from 32 stratospheric whole air samples collected by the NASA ER-2 aircraft between 1997 and 2000 from 62°N to 89°N with N_2O mixing ratios ranging from 51 to 313 ppbv. The relationships between the isotopic compositions and N_2O mixing ratios show significant differences between aircraft deployments and with previous measurements for $N_2O <$ 200 ppbv. The differences between ER-2 deployments at low N_2O are significant at the 3σ level and are due to the effects of transport and mixing. The ratios of enrichment factors for the different isotopologues, however, are the same to within their 1σ uncertainties for $N_2O >$ 200 ppbv and $N_2O <$ 200 ppbv. The observed isotope:N_2O relationships are also used to estimate the fluxes of the N_2O isotopologues from the stratosphere to the troposphere given independent estimates of the N_2O loss rate. On the basis of the robustness of isotope: N_2O relationships for $N_2O >$ 200 ppbv we conclude that the fluxes to the troposphere estimated from these relationships and, therefore, the influence of stratosphere-to-troposphere transport on the isotopic compositions of N_2O in the free troposphere are now relatively well quantified, leaving the isotopic compositions of the N_2O sources as the remaining largest uncertainties in the global N_2O isotope budget. *INDEX TERMS:* 0317 Atmospheric Composition and Structure: Chemical kinetic and photochemical properties; 0322 Atmospheric Composition and Structure: Constituent sources and sinks; 0341 Atmospheric Composition and Structure: Middle atmosphere—constituent transport and chemistry (3334); 1610 Global Change: Atmosphere (0315, 0325); *KEYWORDS:* stratospheric nitrous oxide, isotopic fractionation, global isotope budget

Citation: Park, S., E. L. Atlas, and K. A. Boering (2004), Measurements of N_2O isotopologues in the stratosphere: Influence of transport on the apparent enrichment factors and the isotopologue fluxes to the troposphere, *J. Geophys. Res.*, *109*, D01305, doi:10.1029/2003JD003731.

1. Introduction

[2] Atmospheric N_2O is a long-lived greenhouse gas produced in the troposphere by terrestrial and oceanic biological processes as well as by agriculture and industry [e.g., *Prather and Ehhalt*, 2001]. Photolysis by solar ultraviolet radiation between 185 and 220 nm in the stratosphere is responsible for about 90% of the total N_2O destruction (reaction (R1)). Photo-oxidation by reaction with electronically excited oxygen atoms ($O(^1D)$ in reactions (R2a) and (R2b)) accounts for 10% and is the primary source of nitrogen oxide radicals in the stratosphere which participate in catalytic cycles of ozone destruction.

$$\text{(R1)} \qquad N_2O + h\nu \rightarrow N_2 + O(^1D)$$

$$\text{(R2a)} \qquad N_2O + O(^1D) \rightarrow N_2 + O_2$$

$$\text{(R2b)} \qquad \rightarrow 2NO$$

[3] The current atmospheric N_2O burden is increasing at a rate of ~0.25% per year, reflecting changes in its biogeo-

0148-0227/04/2003JD003731$09.00

chemical cycling. Although the imbalance of sources and sinks is relatively well-quantified, large uncertainties still remain in the various source magnitudes and how they may change over time [e.g., *Bouwman et al.*, 1995; *Kroeze et al.*, 1999; *Mosier et al.*, 1998; *Prather and Ehhalt*, 2001]. Thus, even though N_2O is targeted for emission regulations by the Kyoto Protocol, an incomplete understanding of the global N_2O budget makes establishing an effective regulation strategy difficult.

[4] An additional constraint on the global N_2O budget is a comparision of the distinct isotopic signatures of its sources and sinks, weighted by estimates of the source and sink magnitudes, with isotopic measurements in the free troposphere [e.g., *Kim and Craig*, 1993; *Perez et al.*, 2000; *Yoshida and Matsuo*, 1983; *Yoshida and Toyoda*, 2000]. *Kim and Craig* [1993] first suggested that the return flux of isotopically enriched N_2O from the stratosphere was needed to balance light N_2O from known surface sources to yield the observed ^{15}N and ^{18}O isotopic compositions of N_2O in the free troposphere. Their suggestion was based on two stratospheric measurements which showed significant enrichment in ^{15}N and ^{18}O. Since then, considerable effort has been expended to understand what processes control the enrichment of heavy isotopes in stratospheric N_2O and, in turn, to quantify the influence of the stratospheric fractionation processes on tropospheric N_2O isotopic compositions.

[5] In this paper, we present new measurements of N_2O isotopic compositions on stratospheric air, including $\delta^{18}O$, site-specific $\delta^{15}N$ (i.e., the ^{15}N isotopic composition at the central or terminal position, expressed in this paper as $\delta^{15}N^{\alpha}$ or $\delta^{15}N^{\beta}$, respectively), and $\delta^{15}N^{bulk}$ (i.e., the average of the two N atom positions). These measurements were made on 32 whole air samples collected by the NASA ER-2 aircraft at high latitudes in 1997 and 2000 and significantly enhance the existing stratospheric high-precision, high-accuracy N_2O isotope database of 35 measurements of $\delta^{15}N^{bulk}$ and $\delta^{18}O$ [*Rahn and Wahlen*, 1997; *Röckmann et al.*, 2001; *Toyoda et al.*, 2001] and 28 measurements of $\delta^{15}N^{\alpha}$ [*Röckmann et al.*, 2001; *Toyoda et al.*, 2001]. We report the first observed differences in the N_2O isotopic compositions as a function of N_2O mixing ratio (and thus in apparent enrichment factors) that can be explained entirely by transport and mixing. We analyze the ratios of the observed enrichment factors, which has recently been suggested as a means to quantify the relative contributions of photolysis and photo-oxidation in different regions of the stratosphere [*Kaiser et al.*, 2002a; *Röckmann et al.*, 2001]. Finally, we use the ER-2 measurements to estimate the fluxes of N_2O isotopologues from the stratosphere to the troposphere given independent estimates of the global N_2O loss rate and show that the uncertainty in these fluxes is small (±25%) compared to the uncertainties in the N_2O source fluxes [e.g., *Kroeze et al.*, 1999; *Mosier et al.*, 1998; *Prather and Ehhalt*, 2001]. Thus we argue that the influence of photochemical isotopic fractionation in the stratosphere on free tropospheric N_2O isotope compositions is now well quantified, in agreement with recent two-dimensional (2-D) and 3-D N_2O isotope modeling studies [*Blake et al.*, 2003; *McLinden et al.*, 2003] and analyses of N_2O isotope measurements in firn air [*Röckmann et al.*, 2003a]. The isotopic compositions of the individual N_2O sources are now left as the remaining largest uncertainties in the global N_2O isotope budget.

2. Background and Motivation

[6] After the discovery of isotopically enriched N_2O in the stratosphere by *Kim and Craig* [1993], *Yung and Miller* [1997] proposed that the preferential photolysis of isotopically light N_2O (i.e., $^{14}N^{14}N^{16}O$) is primarily responsible for the significant enrichment of heavy isotopes in the residual N_2O. Their proposed mechanism was that a red shift in the ground state zero point energy (ZPE) of $^{14}N^{14}N^{16}O$ relative to the heavy isotopologues resulted in a red shift of its absorption cross section into a region of the spectrum where more solar photons are available (i.e., the solar window). This theory also explained why *Johnston et al.* [1995], performing photolysis experiments at 185 nm where all N_2O isotopologues show their maximum absorption cross-sections, did not observe significant isotope fractionation for ^{18}O in the laboratory. Although the quantum mechanical details of the Yung and Miller "ZPE" theory continue to be refined, such as including the effects of isotopic substitution on the electronically excited state as well as the ground state [*Johnson et al.*, 2001; *Blake et al.*, 2003], their general mechanism has been verified by subsequent laboratory photolysis experiments performed at wavelengths >185 nm [e.g., *Rahn et al.*, 1998; *Röckmann et al.*, 2000, 2001; *Turatti et al.*, 2000; *Zhang et al.*, 2000; *Kaiser et al.*, 2002b, 2003a].

[7] The experimental photolysis results confirm that the N_2O remaining after photolysis is enriched in all heavy isotopes, in accord with the Rayleigh fractionation equation (equation (1)). This form of the Rayleigh fractionation equation describes the evolution of measured N_2O isotope ratios, R (where $R = {}^{15}N/{}^{14}N$ or ${}^{18}O/{}^{16}O$, for example), as N_2O is destroyed by an irreversible removal process in a well-mixed, closed system.

$$\ln\left(\frac{R}{R_o}\right) = (\alpha - 1) \times \ln\left(\frac{[N_2O]}{[N_2O]_o}\right) \quad (1)$$

R and R_o are the observed and the initial isotope ratios, respectively, and $[N_2O]$ and $[N_2O]_o$ are the observed and initial mixing ratios of N_2O. The fractionation factor, α, is the magnitude of the isotope effect for N_2O destruction. For the photolysis experiments, α is simply the ratio of the photolysis rate coefficients.

$$\alpha = \frac{J'}{J} \quad (2)$$

where J' and J denote the photolysis rate coefficients for one of the heavy isotopologues (e.g., $^{15}N^{14}N^{16}O$, $^{14}N^{15}N^{16}O$, or $^{14}N^{14}N^{18}O$) and the light isotopologue (i.e., $^{14}N^{14}N^{16}O$), respectively. Since α is normally close to unity, for convenience the enrichment factor, ε, is defined as

$$\varepsilon = (\alpha - 1) \cdot 1000. \quad (3)$$

In this paper, we will refer to specific enrichment factors as "$\varepsilon(x)$" where $x = {}^{18}O$, $^{15}N^{\alpha}$, or $^{15}N^{bulk}$ for the enrichment

factors for $^{14}N^{14}N^{18}O$, $^{14}N^{15}N^{16}O$, and the average of $^{15}N^{14}N^{16}O + ^{14}N^{15}N^{16}O$ relative to $^{14}N^{14}N^{16}O$, respectively.

[8] In general, isotope ratios, R, are measured and reported relative to an international isotope reference material using δ notation (equation (4)):

$$\delta = 1000 \cdot (R/R_{STD} - 1) \quad (4)$$

where R_{STD} is the isotope ratio in atmospheric N_2 for $\delta^{15}N$ and Vienna-Standard Mean Ocean Water (V-SMOW) for $\delta^{18}O$. When the δ value is defined as in equation (4), δ is the magnitude of the deviation of the isotope ratio of a sample relative to the ratio of a reference material expressed in "per mil" (effectively parts per thousand) or "‰". Combining equations (3) and (4) with equation (1) yields the Rayleigh fractionation equation expressed in terms of isotopic compositions in δ notation and the enrichment factor, ε (equation (5)).

$$\ln\left(\frac{\delta}{1000}+1\right) - \ln\left(\frac{\delta_o}{1000}+1\right) = \frac{\varepsilon}{1000} \times \ln\left(\frac{[N_2O]}{[N_2O]_o}\right) \quad (5)$$

For an isolated system with constant ε, a plot of isotopic compositions versus $\ln([N_2O]/[N_2O]_o)$ will therefore yield a line with slope equal to ε. (Note that ε is negative for a "normal" isotope effect for which reaction rates are slower for the heavier isotopologues (i.e., for α defined as in equation (3)).)

[9] Laboratory photolysis experiments at different wavelengths have yielded different values for ε [e.g., *Röckmann et al.*, 2000; *Turatti et al.*, 2000; *Zhang et al.*, 2000; *Kaiser et al.*, 2003a]. The *Röckmann et al.* [2000] study, however, also showed that experimental ε values were relatively constant for photolysis with an antimony lamp which approximates stratospheric actinic fluxes at various altitudes quite well. These photolysis experiments yielded ε values of −33.1 ± 0.8 (2σ) ‰ for $\delta^{18}O$, −36.5 ± 1.1‰ for $\delta^{15}N^{bulk}$, and −51.2 ± 1.6‰ for $\delta^{15}N^{\alpha}$. Note that the photolysis-induced fractionation for $^{14}N^{15}NO$ (i.e., $\varepsilon(^{15}N^{\alpha})$) is greater than that for $^{15}N^{14}NO$, resulting in part from the lower zero point energy of the N-O bond in $^{14}N^{15}NO$ [*Yung and Miller*, 1997]. Thus the nitrogen isotopic compositions are different for the central atom position ($^{14}N^{15}NO$) and the terminal nitrogen atom position ($^{15}N^{14}NO$); the overall $\delta^{15}N$ isotopic composition (or "$\delta^{15}N^{bulk}$") is an average of the site-specific isotopic compositions [e.g., *Brenninkmeijer and Röckmann*, 1999].

[10] Recent experiments by *Kaiser et al.* [2002a] have shown that there is also a smaller isotope fractionation due to reaction with $O(^1D)$. They report that all heavy isotopes in the residual N_2O were enriched, yielding values for ε of −12.23 ± 0.14 (2σ) ‰ for $\delta^{18}O$, −5.50 ± 0.19‰ for $\delta^{15}N^{bulk}$, and −2.22 ± 0.12‰ for $\delta^{15}N^{\alpha}$. In contrast to fractionation due to photolysis, enrichment of $^{15}N^{14}NO$ was greater than that for $^{14}N^{15}NO$.

[11] In the stratosphere, which is not an isolated, well-mixed system and in which N_2O destruction by photolysis or by reaction with $O(^1D)$ can both occur, the observed isotope fractionation will not strictly obey a simple Rayleigh fractionation equation. Indeed, the existing stratospheric database of all N_2O isotopic composition observations, composed of measurements by *Kim and Craig* [1993], *Rahn and Wahlen* [1997], *Griffith et al.* [2000], *Yoshida and Toyoda* [2000], *Röckmann et al.* [2001], and *Toyoda et al.* [2001], has demonstrated that most of the values for the apparent enrichment factors, $\varepsilon_{app}(x)$, determined from the observations are smaller by ~50% than those obtained from the N_2O photolysis experiments perfomed both at individual wavelengths [e.g., *Rahn et al.*, 1998; *Turatti et al.*, 2000; *Zhang et al.*, 2000; *Kaiser et al.*, 2003a] and over a range of wavelengths characteristic of stratospheric conditions [*Röckmann et al.*, 2001]. *Rahn et al.* [1998] used a one-dimensional eddy diffusive transport model to explain qualitatively how the experimental values for $\varepsilon(^{15}N^{bulk})$ and $\varepsilon(^{18}O)$ could exceed the values derived from Rayleigh plots of the isotope compositions and N_2O mixing ratios observed in the stratosphere. *Röckmann et al.* [2001] also qualitatively explained the difference between ε values measured in the laboratory and ε_{app} values derived from stratospheric observations as being due to attenuation of ε from transport and mixing, while *Kaiser et al.* [2002a] presented a rigorous 1-D model. In addition, *Röckmann et al.* [2001] noted that destruction of N_2O by reaction with $O(^1D)$ could also contribute to the smaller observed values for ε than those from experiment. *Toyoda et al.* [2001] raised similar points. Confirming their qualitative transport and mixing explanations, *McLinden et al.* [2003] used a 3-D chemical transport model to simulate the distribution of N_2O isotopologues in the stratosphere and noted that simulations using a more diffusive meteorology (GISS II') produced smaller ε_{app} values than a more advective one (GISS II). Thus, using the same model photochemistry and kinetic isotope effects, the more diffusive the model transport is (i.e., the more transport and mixing there is), the more attenuated the resulting ε_{app} values are, as expected.

[12] The balloon observations of both *Röckmann et al.* [2001] and *Toyoda et al.* [2001] also showed that values for ε_{app} varied significantly between low and high N_2O mixing ratios [*Röckmann et al.*, 2001] or, approximately equivalently for vertical profiles from balloon platforms, between high and low altitudes [*Toyoda et al.*, 2001], respectively. Differences in slopes derived from the data plotted in Rayleigh format (equation (5)) as large as 30 to 50% were found for N_2O mixing ratios above and below 200 nmol/mol (hereinafter referred to as ppbv of dry, ideal air) [*Röckmann et al.*, 2001] or for altitudes above and below ~ 24 km. [*Toyoda et al.*, 2001] (see Table 1). The cause or causes for these observed differences in ε_{app} as a function of N_2O or altitude have been debated, and the following potential mechanisms have been discussed: (1) differences in the attenuation of the chemistry-only ε due to characteristically different transport or mixing in different regions of the stratosphere [*Röckmann et al.*, 2001; *Toyoda et al.*, 2001], (2) dependence of the ε on photolysis wavelength and/or temperature and therefore altitude [*Röckmann et al.*, 2001; *Toyoda et al.*, 2001], and (3) the relatively larger contribution of the reaction with $O(^1D)$ in the lower stratosphere to total N_2O destruction in that region [*Röckmann et al.*, 2001; *Toyoda et al.*, 2001; *Kaiser et al.*, 2002a].

[13] Several experimental studies have addressed item 2 above. In their antimony lamp photolysis experiment, *Röckmann et al.* [2001] found no difference in enrichment factors between photolysis using the full spectrum of the

Table 1. Enrichment Factors and Their Ratios for N_2O Isotopologues From Laboratory Experiments and From Individual Data Sets of Stratospheric Observations

	Enrichment Factor[a]				Ratio of Enrichment Factors[b]			
	$\lvert\varepsilon^{bulk}\rvert$	$\lvert\varepsilon^{\alpha}\rvert$	$\lvert\varepsilon^{\beta}\rvert$	$\lvert\varepsilon^{18}\rvert$	$\varepsilon^{\alpha}/\varepsilon^{bulk}$	$\varepsilon^{bulk}/\varepsilon^{18}$	$\varepsilon^{\alpha}/\varepsilon^{18}$	$\varepsilon^{\alpha}/\varepsilon^{\beta}$
Laboratory experiments								
Photolysis	36.5 (±1.1)	51.2 (±1.6)	21.4 (±1.1)	33.1 (±0.8)	1.40 (±0.06)	1.10 (±0.04)	1.55 (±0.06)	2.39 (±0.14)
$O(^1D)$ reaction	5.50 (±0.19)	2.22 (±0.12)	8.79 (±0.15)	12.23 (±0.14)	0.40 (±0.02)	0.45 (±0.01)	0.18 (±0.01)	0.25 (±0.01)
Toyoda et al. [2001][b]								
>24.1 km	28.6 (±1.2)	40.9 (±2.6)	15.5 (±0.8)	24.6 (±1.2)	1.43 (±0.11)	1.16 (±0.07)	1.66 (±0.13)	2.64 (±0.22)
<24.1 km	15.9 (±2.2)	22.9 (±2.4)	8.8 (±2.8)	11.5 (±3.6)	1.44 (±0.25)	1.38 (±0.47)	1.99 (±0.66)	2.60 (±0.87)
Röckmann et al. [2001][b,c]								
All	24.3 (±0.7)	32.3 (±1.2)	16.0 (±0.6)	21.0 (±0.6)	1.33 (±0.06)	1.16 (±0.05)	1.54 (±0.07)	2.02 (±0.11)
>200 ppbv	16.8 (±1.6)	20.9 (±1.5)	12.7 (±2.4)	13.8 (±2.0)	1.24 (±0.15)	1.22 (±0.21)	1.51 (±0.24)	1.64 (±0.33)
Rahn and Wahlen [1997][d]								
>185 ppbv	14.5	-	-	12.9	-	1.12	-	-
This work ER-2[e]								
<200 ppbv SOLVE	24.3 (±0.8)	35.0 (±2.7)	13.1 (±2.2)	20.6 (±1.4)	1.44 (±0.06)	1.18 (±0.03)	1.70 (±0.07)	2.60 (±0.44)
<200 ppbv POLARISII	14.9 (±4.9)	18.7 (±9.0)	11.0 (±1.7)	13.4 (±4.3)	1.32 (±0.19)	1.20 (±0.06)	1.58 (±0.21)	1.79 (±0.85)
<200 ppbv All	22.1 (±4.2)	30.8 (±6.4)	12.9 (±3.0)	18.9 (±3.5)	1.41 (±0.06)	1.17 (±0.03)	1.65 (±0.06)	2.35 (±0.34)
>200 ppbv All	14.9 (±1.1)	22.4 (±2.5)	7.1 (±2.9)	13.3 (±0.9)	1.51 (±0.12)	1.12 (±0.04)	1.70 (±0.17)	2.65 (±0.99)

[a]The values are given in ‰; 2σ uncertainties are given in parentheses and throughout the text. All ε values from previous studies cited here are from the original publications.

[b]The ratios of ε shown here for the *Toyoda et al.* [2001] and *Röckmann et al.* [2001] data sets were calculated in the original publications by taking the ratio of ε values derived individually from Rayleigh plots for the different N_2O or altitude ranges noted. Ratios shown in the figures and discussed in the text, however, are all computed from regressions of $\ln(\delta^x/1000 + 1) - \ln(\delta_o^x/1000 + 1)$ versus $\ln(\delta^y/1000 + 1) - (\delta_o^y/100 + 1)$; see section 4.

[c]Published fractionation constants (denoted as E here) were defined as $E = k/k' - 1$, for which $\varepsilon = -E/(1 + E)$; for consistency, the E values were converted to ε values here.

[d]Values given by the authors for WB-57 aircraft samples between 33°N and 48°N.

[e]The ratios of ε values given are from geometric mean regressions of the ln-ln relationship given in footnote b above.

lamp (184–225 nm) and when adding an interference filter that transmitted only 207 ± 10 nm light; these results suggest that a significant shift in photolysis wavelength within the solar window does not cause a detectable change in the overall enrichment factor. Recent experiments on the specific wavelength dependence of ε values [*Kaiser et al.*, 2003a] confirmed this conclusion. The temperature dependence of isotopic fractionation during N_2O photolysis has been investigated experimentally by *Kaiser et al.* [2002b]. This work revealed that the enrichment factors are larger at lower temperatures. Hence, the enrichment factors would decrease with altitude, not increase as observed.

[14] To address item 3 in the list above, an additional constraint on the relative contributions of photolysis versus reaction with $O(^1D)$ in different regions of the stratosphere and their effect on isotopic compositions has been proposed by *Röckmann et al.* [2001] and discussed further in *Kaiser et al.* [2002a]. They proposed that the ratios of enrichment factors (e.g., $\varepsilon(^{15}N^{\alpha})/\varepsilon(^{15}N^{\beta})$, $\varepsilon(^{15}N^{bulk})/\varepsilon(^{18}O)$, etc.) would not be significantly affected by transport and could therefore potentially be used to resolve changes in the overall isotopic fractionation due to photolysis or reaction with $O(^1D)$ in different regions of the stratosphere. Motivated in part by this idea, *Kaiser et al.* [2002a] measured oxygen and site-specific nitrogen enrichment factors for $N_2O + O(^1D)$ in the laboratory and showed that the ratios $\varepsilon(^{15}N^{\alpha})/\varepsilon(^{15}N^{\beta})$, $\varepsilon(^{15}N^{\alpha})/\varepsilon(^{15}N^{bulk})$, $\varepsilon(^{15}N^{bulk})/\varepsilon(^{18}O)$, and $\varepsilon(^{15}N^{\alpha})/\varepsilon(^{18}O)$ are 0.25, 0.40, 0.45, and 0.18, respectively, and are distinctly different from the ratios of 2.39, 1.40, 1.10, and 1.55 for photolysis. Both *Röckmann et al.* [2001] and *Toyoda et al.* [2001] derived ε values from plots of $\ln(\delta/1000 + 1)$: $\ln([N_2O]/[N_2O]_o)$ for N_2O mixing ratios above and below 200 ppbv or altitudes above and below 24.1 km, respectively, and then took the ratios of $\varepsilon(^{15}N^{\alpha})$ and $\varepsilon(^{15}N^{\beta})$ or $\varepsilon(^{15}N^{bulk})$ and $\varepsilon(^{18}O)$ for these two different regimes. *Röckmann et al.* [2001] argued that the values for $\varepsilon(^{15}N^{\alpha})/\varepsilon(^{15}N^{\beta})$ also change at ~200 ppbv N_2O, just as the enrichment factors themselves vary with N_2O mixing ratio or altitude. Although the observed differences in the values for the ratio $\varepsilon(^{15}N^{\alpha})/\varepsilon(^{15}N^{\beta})$ are not statistically significant at the 2σ level (see, e.g., Table 1 or our geometric mean regression analysis of their data yielding ratios of 2.03 ± 0.12 (2σ) versus 1.68 ± 0.36 (2σ) for $N_2O < 200$ ppbv and $N_2O > 200$ ppbv), *Röckmann et al.* [2001] and *Kaiser et al.* [2002a] speculated that either an increasing proportion of N_2O loss in the lower stratosphere by reaction with $O(^1D)$ or, alternatively, some other source(s) of N_2O in the stratosphere might be responsible for the difference in $\varepsilon(^{15}N^{\alpha})/\varepsilon(^{15}N^{\beta})$ values between low and high N_2O mixing ratios.

[15] Recent N_2O isotope modeling studies have attempted to provide additional insight into the underlying causes for changes in the observed enrichment factors and/or ratios of enrichment factors between high- and low-N_2O-mixing-ratio regimes. *McLinden et al.* [2003] calculated photolysis Rayleigh curves from the mean of the modeled J-values for photolysis (on the basis of the overall lifetimes of the N_2O isotopologues in their model). They found that the Rayleigh curves remained linear in their model and interpreted this to mean that transport was solely responsible for the modeled changes in ε_{app} values as a function of N_2O mixing ratio or altitude. However, even though the calculated isotope-specific photolysis cross-sections used in their model included their temperature and wavelength dependence [from *Johnson et al.*, 2001], use of the mean of the J-values over the entire stratosphere to calculate Rayleigh curves means that changes in the isotope-specific photolysis rates as a function of latitude

and/or altitude could still contribute to observed and modeled changes in ε_{app} values as a function of N_2O mixing ratio or altitude. Moreover, *McLinden et al.* [2003] did not examine simulated ratios of enrichment factors in different regions of the stratosphere nor did they have recent experimental values for $\varepsilon(^{15}N^{\alpha})$, $\varepsilon(^{15}N^{\beta})$, and $\varepsilon(^{15}N^{bulk})$ for the reaction $N_2O + O(^1D)$ from *Kaiser et al.* [2002a]. In their 2-D model, *Morgan et al.* [2003] did compare the ratios of $\varepsilon_{app}(^{15}N^{\alpha})/\varepsilon_{app}(^{15}N^{\beta})$ in the lower stratosphere (where the relative contribution of $O(^1D)$ to the total N_2O sink is greater) with and without including fractionation by $O(^1D)$. They found little to no difference in the ratios of enrichment factors. However, they did not examine the effect of removing the $O(^1D)$ sink completely but, rather, they compared model runs using an $O(^1D)$ KIE of 1.000 versus model runs using the new experimental values for the $O(^1D)$ KIE from *Kaiser et al.* [2002a], ranging from 1.012 to 1.002 for $\varepsilon(^{18}O)$ and $\varepsilon(^{15}N^{\alpha})$, respectively. Without comparing the ratios of ε values with and without the $O(^1D)$ sink, little difference would be expected in any case. Hence, this simulation does not rigorously test the suggestion of *Röckmann et al.* [2001] and *Kaiser et al.* [2002a] that an increase in the relative contribution of reaction with $O(^1D)$ to the total N_2O sink in the lower stratosphere results in an observable decrease in the ratio in the lower stratosphere compared to the middle stratosphere.

[16] In light of these remaining uncertainties, additional N_2O isotope observations at different times and locations in the stratosphere, particularly new site-specific $\delta^{15}N^{\alpha}$ isotopic compositions, should provide further information and constraints on what controls the variation of enrichment factors as a function of N_2O mixing ratio and/or altitude. The 32 measurements on air samples from the ER-2 aircraft are highly complementary to the existing high-precision, high-accuracy stratospheric N_2O isotope database and nearly double the number of available measurements of $\delta^{18}O$ and $\delta^{15}N^{bulk}$ (8 from *Rahn and Wahlen* [1997], 16 from *Röckmann et al.* [2001], and 11 from *Toyoda et al.* [2001]; we note here that the 2 data points of *Kim and Craig* [1993] are suspect because of CO_2 contamination as noted by *Rahn and Wahlen* [1997], that the infrared spectroscopic measurements of *Griffith et al.* [2000] are less precise than mass spectrometric measurements, and that the four points of *Yoshida and Toyoda* [2000] are likewise not included in the analyses of *Toyoda et al.* [2001]). Samples were collected in the lower stratosphere but also include some samples of air characteristic of higher altitudes that has descended in the polar vortex with mean ages up to 6 years [e.g., *Andrews et al.*, 2001]. A large number of other tracer and meteorological measurements were made on the aircraft and have been studied extensively, providing important information on the chemical and dynamical context of the sampled air. Moreover, since lower stratospheric air is the source of isotopically enriched N_2O to the troposphere, observations from the ER-2 observations are presented and compared with other stratospheric observations made to date. In section 5, the observations and their implications are discussed, and estimates of the fluxes of heavy N_2O isotopologues from the stratosphere to the troposphere are made based solely on observations and independent estimates of the N_2O loss rate in the stratosphere.

3. Experimental Details

3.1. Sample Collection and Measurement of Trace Gas Mixing Ratios

[17] Whole air samples were collected with the National Center for Atmospheric Research (NCAR) Whole Air Sampler (WAS) [*Flocke et al.*, 1999] on board the NASA ER-2 aircraft during the Photochemistry of Ozone Loss in the Arctic Region in Summer (POLARIS) mission from April to September 1997 [*Newman et al.*, 1999] and the SOLVE mission (Stratospheric Aerosol and Gas Experiment (SAGE) III Ozone Loss and Validation Experiment) from January to March 2000 [*Newman et al.*, 2002]. The deployments allowed for substantial sampling in the Arctic vortex in the winter of 2000, during vortex break-up in April 1997, and in the Arctic region in the spring, summer, and early fall from May through September 1997.

[18] The WAS instrument consisted of 28 (POLARIS) to 40 (SOLVE) 1.6-liter electropolished stainless steel canisters, a 4-stage metal bellows pump, a stainless steel manifold, motor-driven valves, and an electronics package for valve and pump control. The metal bellows pump pressurized the instrument manifold to 40 psia (2.7 bar), resulting in a sample volume of ~4.5 standard liters (STP). The filling time varied with flight altitude, ranging from 15 to ~180 s. After sample collection, the canisters were transported to NCAR and analyzed in the laboratory. The mixing ratios of approximately 50 different species were measured by gas chromatography-mass spectrometry.

[19] Measurements of N_2O mixing ratios on the SOLVE whole air samples were made using an HP5890 II+ series GC fitted with an electron capture detector (ECD) relative to a 314 ppbv N_2O secondary standard of whole air calibrated against a 300 nmol/mol National Institute Standards and Technology (NIST) SRM (2608, ±1%) reference gas. The average uncertainty (2σ) for the N_2O mixing ratio data is less than 0.7 ± 0.1% [*Hurst et al.*, 2002]. For POLARIS, N_2O was not measured on the whole air samples collected during the campaign, so in this study we use N_2O mixing ratios measured in situ on the ER-2 by the Airborne Tunable Diode Laser Spectrometer (ATLAS) [*Podolske and Loewenstein*, 1993; see also *Hurst et al.*, 2000]. The in situ N_2O data were averaged over the sample collection period weighted by the canister-filling rate. Both in-flight and laboratory calibrations for the ATLAS instrument were performed with a suite of reference gases tied to the NOAA/CMDL N_2O calibration scale. The reported precision and accuracy of the ATLAS instrument are ±1.5% and ±2.5%, respectively [*Hurst et al.*, 2000].

[20] In this study, we also rely on CH_4 mixing ratios measured on the WAS samples. Mixing ratios of CH_4 on the whole air samples from both missions were measured using a Hewlett Packard model 5890 gas chromatograph fitted with a flame ionization detector (GC-FID). Calibration was

made against a 0.913 ± 0.01 and a 1.19 ± 0.01 μmol/mol NIST-certified SRM 1658a reference gas. Measurement precision is ±10 ppbv (1σ) and accuracy is ±20 ppbv (1σ).

3.2. Isotopic Measurements

[21] After the trace gas mixing ratios were measured at NCAR by GC-MS, ~2 to 4 liters (STP) of sample remained for isotopic analyses. Approximately half of each remaining sample was transferred on a vacuum line to an evacuated (10^{-5} hPa) archival 1.5-liter Pyrex flask with a Loeuwers-Hapert glass valve and Viton o-rings for measurements of the isotopic compositions of N_2O, CH_4 [*Rice et al.*, 2003; *McCarthy et al.*, 2003], H_2 [*Rahn et al.*, 2003], and $\delta^{15}N$ of N_2 and $\delta^{18}O$ of O_2 (see section 3.2.1). For the other half of the remaining WAS sample, CO_2 was cryogenically separated and stored in a glass ampoule for measurements of $\delta^{18}O$, $\delta^{17}O$ and $\delta^{13}C$ of CO_2.

3.2.1. Isotopic Measurements for Sample Collection and Storage Integrity

[22] Measurements of $\delta^{15}N$ of N_2 and of $\delta^{18}O$ of O_2 were made at Princeton University (M. Bender, personal communication, 2002). In the absence of gravitational fractionation, shifts in the isotopic composition of N_2 or O_2 relative to their known constant values in the troposphere would indicate significant mass fractionation of the whole air samples at some point in the collection and storage history. While the samples do appear to be slightly fractionated, there is no anti-correlation of the $\delta^{15}N$ of N_2 measurements with the WAS N_2O mixing ratios. Such a correlation might have indicated a detectable degree of gravitational fractionation occurring in (or transported into) the stratosphere, although turbulence is expected to prevent gravitational fractionation from occurring below altitudes of 100 km [e.g., *Brasseur and Solomon*, 1986]. Rather, for our purposes here, these measurements serve as a test of the integrity of the WAS sample collection and storage schemes for preserving the isotopic compositions of the sampled air. The upper limit on fractionation artifacts due to sample collection and transfer provided by the $\delta^{15}N$ of N_2 and $\delta^{18}O$ of O_2 measurements is 0.1‰ for $\delta^{15}N$ of N_2O, on the order of the measurement precision for both N_2O isotopes; hence, this fractionation can be ignored in the analysis presented here.

3.2.2. Isotopic Measurements for N_2O

[23] For this study, 32 WAS samples were analyzed for $\delta^{15}N^{bulk}$, site-specific $\delta^{15}N^{\alpha}$ (or the isotopic composition at the central atom in N_2O) and $\delta^{18}O$ of N_2O. Samples ranged in latitude from 62°N and 88°N and in altitude from 11 to 21 km and were collected in April 1997 (“POLARIS I”), June and July 1997 (“POLARIS II”), September 1997 (“POLARIS III”), and January, February, and March 2000 (“SOLVE”). These samples were selected from approximately 400 samples archived at University of California, Berkeley (UC Berkeley), based solely on collection latitudes >60°N and N_2O mixing ratios spanning the widest range possible. The measurements were performed at UC Berkeley using a Finnigan MAT 252 isotope ratio mass spectrometer operated in continuous flow mode coupled with an online Finnigan preconcentrator and gas chromatograph [e.g., *Brand*, 1995]. Aliquots of 100 to 400 ml (STP; equivalent to 0.8–1.4 nmol of N_2O, depending on N_2O mixing ratio and flask pressure) were taken by expanding the sample in the archival 1.5-liter Pyrex flask into an evacuated (10^{-5} hPa) two-valved Pyrex analysis flask and then isolating each flask. Two separate aliquots were required for (1) the $\delta^{15}N^{bulk}$ and $\delta^{18}O$ measurements and (2) the site-specific $\delta^{15}N^{\alpha}$ measurement.

[24] Each two-valved analysis flask containing an aliquot of a whole air sample was then attached to the preconcentrator/GC/IRMS system. For $\delta^{15}N^{bulk}$ and $\delta^{18}O$, the N_2O^+ molecular ions at mass to charge (m/*z*) values of 44, 45 and 46 were measured. For site-specific $\delta^{15}N^{\alpha}$, the NO^+ fragment ion at m/*z* values of 30 and 31 were measured [e.g., *Brenninkmeijer and Röckmann*, 1999; *Toyoda and Yoshida*, 1999]. The isotope ratios ($^{15}N/^{14}N$ and $^{18}O/^{16}O$ for the molecular ion and the site-specific $^{15}N/^{14}N$ ratio for the NO^+ fragment ion) were measured relative to those of a pure N_2O reference gas (i.e., our laboratory working standard; Scott Specialty Gases, 99.998%).

[25] For $\delta^{15}N^{bulk}$ and $\delta^{18}O$ measurements, our laboratory working standard was calibrated using a dual inlet IRMS (Finnigan MAT model 252) in the Brenninkmeijer group at the Max Planck Institute for Air Chemistry in Mainz against their laboratory reference gas, which was calibrated against the international air-N_2 and V-SMOW isotope reference materials, respectively [*Kaiser*, 2002]. On the basis of these intercomparisons, the UC Berkeley N_2O working standard has an average ^{15}N isotopic composition of $\delta^{15}N^{bulk} = 0.07 \pm 0.06$‰ (1σ, 5 analyses) relative to air-N_2 and an ^{18}O isotopic composition of $\delta^{18}O = 41.55 \pm 0.20$‰ (n = 5) relative to V-SMOW.

[26] For the site-specific isotopic compositions $\delta^{15}N^{\alpha}$ and $\delta^{15}N^{\beta}$, calibration to a common isotope scale for comparisons between data sets is more difficult. The first difficulty is that the NO^+ fragment ions within the IRMS are unfortunately not formed exclusively by loss of the terminal nitrogen (i.e., the nitrogen atom in the β position) of the parent molecular ion N_2O^+ [e.g., *Brenninkmeijer and Röckmann*, 1999]; an ion rearrangement (or “scrambling”) process can occur, most likely because of the formation of triangular, energetic N_2O^+ ions, which can then decompose by the breaking of either of the two N-O bonds, yielding NO^+ ions which can contain either the terminal or central nitrogen atoms from the N_2O^+ [*Begun and Landau*, 1961]. The determination of the scrambling factor (i.e., the fraction of the NO^+ fragment ions bearing the terminal nitrogen of the initial N_2O to total NO^+ produced) in our Berkeley IRMS was made in a manner similar to that of *Toyoda and Yoshida* [1999]. Three different samples of pure N_2O gas were made by adding small amounts of either $^{14}N^{15}NO$ or $^{15}N^{14}NO$ (both with a ^{15}N atom purity of 99%) to our N_2O working standard. For the three samples, ~0.05 μmol of $^{14}N^{15}NO$, ~0.2 μmol of $^{14}N^{15}NO$, and ~0.06 μmol of $^{15}N^{14}NO$ were added to ~280 μmol N_2O of our working standard in 15-ml glass flasks. One additional 15-ml sample flask contained only the pure N_2O working standard gas. The isotope ratios at m/*z* 30 and 31 for each of the 4 samples were measured against our working standard in the dual inlet mode of the IRMS. The exact amount of the labeled N_2O in each sample was determined by measuring the ion signal at m/*z* 45. For comparison, *Toyoda and Yoshida* [1999] determined the amount of labeled N_2O in the sample manometrically. The scrambling factor was 8.04% in our instrument (This value includes a correction for the purity of

our labeled N_2O; see *Kaiser et al.* [2003b]). Similar values have been measured by other groups on other mass spectrometers: 8.52% by *Begun and Landau* [1961], 8.5% by *Brenninkmeijer and Röckmann* [1999], 8.11% by *Toyoda and Yoshida* [1999] and 8.5% by *Röckmann et al.* [2003b].

[27] Once the scrambling factor is determined, there is additional difficulty in placing the measurements that were made relative to the laboratory working standard onto the international air-N_2 isotope scale [*Toyoda and Yoshida*, 1999]. Details of a purely mass spectrometric technique devised at MPI-Mainz and UC Berkeley to convert site-specific isotope measurements to the air-N_2 scale appear elsewhere [*Kaiser et al.*, 2003b]. However, discrepancies between the Mainz, UC Berkeley, and Tokyo Institute of Technology groups have yet to be completely resolved. Fortunately, because values for the $\delta^{15}N^{bulk}$ and $\delta^{18}O$ isotopic compositions of tropospheric N_2O from *Röckmann et al.* [2001] and *Toyoda et al.* [2001] agree with those measured at UC Berkeley (see below) to within the stated 2σ and 1σ measurement precisions, respectively, tropospheric N_2O can serve as an accurate secondary standard. We therefore report the new ER-2 site-specific $\delta^{15}N$ measurements relative to tropospheric N_2O so that accurate comparisons (to within 2‰) can be made with the Röckmann et al. and Toyoda et al. data sets.

[28] In addition to our measurement accuracy relative to air-N_2, V-SMOW, and tropospheric N_2O for $\delta^{15}N^{bulk}$, $\delta^{18}O$, and $\delta^{15}N^{\alpha}$, respectively, both short-term and long-term measurement precision in our laboratory have been determined. Short-term precision is based on the standard deviations of multiple runs (>5 runs) of a given sample in a single day: $\delta^{15}N^{bulk} = \pm 0.2‰$, $\delta^{18}O = \pm 0.2‰$, and $\delta^{15}N^{\alpha} = \pm 0.8‰$. A number of experimental control runs were performed to check our long-term precision. Long-term measurement precisions for $\delta^{15}N^{bulk}$, $\delta^{15}N^{\alpha}$, and $\delta^{18}O$ were evaluated by monitoring N_2O isotopes in air samples ($\sim$100 ml STP; containing $\sim$1.35 nmol N_2O) taken at the ground level on the UC Berkeley campus. This sampling and measurement routine provided an indication of overall (internal and external) measurement precision over a long time period (October 2001 to September 2002). The measurements were performed against our laboratory working standard discussed earlier, yielding $\delta^{15}N^{bulk} = 6.3 \pm 0.3‰$ versus air-N_2 (1σ; n = 84), $\delta^{18}O = 44.4 \pm 0.3‰$ versus V-SMOW (n = 84), $\delta^{15}N^{\alpha} = 14.7 \pm 0.8‰$ versus UCB working standard (n = 75) with no discernable trend. Therefore we conclude that the long-term measurement precision on whole air samples containing $\sim$1.35 nmol of N_2O is ±0.3‰ for $\delta^{15}N^{bulk}$ and $\delta^{18}O$ and ±0.8‰ for $\delta^{15}N^{\alpha}$.

[29] An additional source of measurement error on our stratospheric samples not constrained by the control runs on 100 ml STP tropospheric samples is the dependence of the measurement precision on the GC peak area and, therefore, on sample size [*Merritt and Hayes*, 1994]. For example, our measurement precision for $\delta^{15}N$ and $\delta^{18}O$ for control runs of tropospheric air in whole air samples of varying sizes were ±0.15‰ and ±0.20‰, respectively, for samples with $N_2O >$ 1.5 nmol. For samples containing smaller amounts of N_2O, however, the precision worsened exponentially with decreasing N_2O. In order to obtain precisions better than ± 0.30‰ for $\delta^{15}N^{bulk}$, ±0.35‰ for $\delta^{18}O$, and ±0.85‰ for $\delta^{15}N^{\alpha}$ on samples with N_2O mixing ratios which varied from 51 to 313 ppbv, the volume of the aliquot for each stratospheric WAS sample run was chosen so that the total amount of N_2O was almost always >1.0 nmol; these varied from 100 to 400 ml. The estimated precision for each stratospheric WAS sample measurement, reported here as error bars in the figures, was determined by noting the GC peak area for each measurement and using the relationship between peak area and precision from our control runs of various N_2O sample sizes. We also note that for our instrument and sample sizes the measured delta values are independent of sample size, so that a correction term for a dependence of delta value on sample size as in the paper by *Röckmann et al.* [2003b] is not necessary.

4. Stratospheric Observations and Analysis

[30] Measurements of $\delta^{15}N^{bulk}$, $\delta^{15}N^{\alpha}$, and $\delta^{18}O$ of N_2O in 32 stratospheric whole air samples from the ER-2 aircraft are summarized in Table 2 and plotted against N_2O mixing ratios in Figure 1, along with measurements on samples collected from the WB-57 aircraft [*Rahn and Wahlen*, 1997] and from balloon platforms [*Röckmann et al.*, 2001; *Toyoda et al.*, 2001]. Note that since tropospheric N_2O mixing ratios reported for the respective data sets are all between 316 and 320 ppbv, a variation on the order of the N_2O analytical precisions, no correction for the atmospheric N_2O increase between 1988 and 2000 was made. For all 4 sets of aircraft and balloon observations, the heavy isotopes of N_2O become enriched as N_2O decreases. The enrichment for $\delta^{15}N^{\alpha}$ (Figure 1b) is greater than that for $\delta^{15}N^{bulk}$ (Figure 1a), in accord with theoretical and laboratory predictions cited in section 2. While this difference in $\delta^{15}N^{bulk}$ and $\delta^{15}N^{\alpha}$ values for a given N_2O mixing ratio was apparent from the separate Toyoda et al. and Röckmann et al. balloon data sets, Figure 1b is the first intercomparison of $\delta^{15}N^{\alpha}$ observations from different groups relative to $\delta^{15}N^{\alpha}$ of tropospheric N_2O, a comparison which should be robust to better than 2‰ on the basis of tropospheric measurements (see section 3.2.2).

[31] Importantly, all the isotope observations for N_2O mixing ratios >200 ppbv, whether measured from balloon or aircraft platforms, show nearly identical compact correlations between the isotopic compositions and N_2O mixing ratios (i.e., the $\delta^{15}N^{bulk}$:N_2O, $\delta^{15}N^{\alpha}$:N_2O, and $\delta^{18}O$:N_2O relationships). Even on a higher-resolution scale than shown in Figure 1, there is no discernable difference between data sets for N_2O mixing ratios >200 ppbv that is larger than the measurement precision and accuracy.

[32] For $N_2O < 200$ ppbv, however, the observed isotope:N_2O relationships exhibit considerable variability. While the ER-2 isotope observations for $N_2O < 200$ ppbv from the SOLVE and POLARIS I campaigns are similar to each other, the POLARIS II data points are significantly different. At $\sim$80 ppbv N_2O, for example, $\delta^{15}N$ for POLARIS II is almost 11‰ lighter than that for the POLARIS I/SOLVE data, a value an order of magnitude larger than the measurement uncertainty. The POLARIS II samples were collected in summer between 29 June and 10 July 1997 while the POLARIS I and SOLVE samples were collected in the Arctic vortex in April 1997 and between January and March 2000, respectively. In section 5, we detail how these differences in the isotope:N_2O relationships within the ER-2 data

Table 2. Isotopic Compositions of Stratospheric N_2O From the NASA ER-2 Aircraft

Flight Date	Latitude, °N	Pressure Altitude, km	Potential Temperature, K	N_2O, ppbv	$\delta^{15}N^{bulk}$, ‰ Air-N_2	$\delta^{18}O$, ‰ VSMOW	$\delta^{15}N^{\alpha}$, ‰ Versus Tropospheric N_2O	$\delta^{15}N^{\beta}$, ‰ Versus Tropospheric N_2O
				POLARIS I				
26 April 1997	80.8	19.1	502.8	225.0	12.1	49.1	8.5	2.9
26 April 1997	84.3	19.2	505.9	139.7	21.2	57.1	22.8	6.5
26 April 1997	87.4	19.0	502.2	107.9	25.4	60.8	30.1	7.4
26 April 1997	87.9	16.7	444.1	207.9	12.9	50.0	10.1	2.8
				POLARIS II				
29 June 1997	62.0	20.8	528.5	83.3	27.7	62.6	30.6	11.5
30 June 1997	64.3	18.7	479.0	257.4	9.6	47.0	5.9	0.6
30 June 1997	62.9	20.5	517.8	103.1	25.1	60.7	28.7	8.2
30 June 1997	65.8	20.5	521.6	104.2	23.0	58.2	23.6	9.2
7 July 1997	88.5	17.2	454.9	267.3	9.3	46.6	3.6	2.4
7 July 1997	75.0	20.5	533.3	78.7	24.5	59.8	24.6	11.2
7 July 1997	73.1	20.5	534.9	134.4	16.7	53.3	15.6	4.8
10 July 1997	63.6	21.1	532.0	154.8	17.5	53.7	18.1	3.8
				POLARIS III				
15 Sept. 1997	64.6	19.4	487.0	226.3	11.9	49.3	8.6	2.5
15 Sept. 1997	65.0	19.4	485.5	205.8	12.5	49.7	9.6	2.5
15 Sept. 1997	64.7	16.7	432.7	288.8	7.7	45.5	2.1	0.7
15 Sept. 1997	64.8	13.3	373.9	313.0	7.2	44.6	0.6	1.1
18 Sept. 1997	78.5	19.3	490.2	185.9	13.7	49.3	11.9	2.6
				SOLVE				
23 Jan. 2000	63.3	17.6	410.7	211.0	12.8	50.2	8.0	4.9
23 Jan. 2000	64.0	13.3	349.3	299.8	7.2	44.8	1.3	0.4
23 Jan. 2000	64.5	11.2	314.4	313.6	6.5	44.4	0.1	0.4
27 Jan. 2000	62.9	20.4	457.2	100.0	29.2	63.6	31.8	13.2
27 Jan. 2000	64.3	20.2	450.2	130.4	23.2	58.4	23.5	9.8
27 Jan. 2000	66.3	20.2	445.0	138.5	21.8	56.3	22.4	8.0
2 Feb. 2000	64.4	18.8	431.6	149.3	19.9	55.8	20.9	5.9
3 Feb. 2000	68.8	17.7	407.8	188.3	15.2	52.4	12.1	5.3
5 March 2000	68.2	16.8	386.7	241.3	10.4	48.4	5.6	2.5
5 March 2000	70.3	18.9	420.6	172.0	16.5	52.8	14.9	5.1
11 March 2000	64.4	18.8	435.4	114.4	25.9	60.3	26.1	12.5
11 March 2000	60.5	17.2	421.8	279.2	8.2	45.8	3.0	0.8
11 March 2000	68.3	19.7	449.6	81.8	35.1	68.9	39.1	17.6
11 March 2000	69.1	20.0	455.8	62.6	42.3	74.9	50.7	20.2
11 March 2000	72.0	20.2	461.1	51.8	46.9	80.0	60.3	19.6

set can be explained entirely by mixing and transport. Differences in the isotope:N_2O relationships between the tropics, midlatitudes, and high latitudes can also be discerned and can be explained at least to first order by transport and mixing (see below).

[33] In Figure 2, the observations of $\delta^{15}N^{bulk}$ of N_2O shown in Figure 1a are plotted in the Rayleigh format of equation (5). As discussed in section 2, the slope of a line fit to the data plotted in this format gives the apparent enrichment factor, $\varepsilon_{app}(^{15}N^{bulk})$. As noted in previous studies [*Griffith et al.*, 2000; *Röckmann et al.*, 2001; *Toyoda et al.*, 2001], it is clear that $\varepsilon_{app}(^{15}N^{bulk})$ is not constant over the range of N_2O sampled. For $N_2O > 200$ ppbv, $\varepsilon_{app}(^{15}N^{bulk})$ is -16.2 ± 1.3 (2σ) ‰ when observations from all the aircraft and balloon data sets are included. In contrast, the values for $\varepsilon_{app}(^{15}N^{bulk})$ for $N_2O < 200$ ppbv reveal considerable variation between data sets as a function of latitude and/or ER-2 deployment, ranging from -14.9 ± 4.9‰ for the ER-2 POLARIS II high-latitude data to -28.6 ± 1.2‰ for the balloon midlatitude data of *Toyoda et al.* [2001]. In fact, on the basis of the slopes of the observations in the Rayleigh format of Figure 2, we note that the POLARIS II data for $N_2O < 200$ ppbv are significantly different from the POLARIS I/SOLVE and balloon data sets for $N_2O < 200$ ppbv at the 3.29σ level (corresponding to the 99.9% confidence interval). Similar trends in the apparent enrichment factors for $\delta^{15}N^{\alpha}$ and $\delta^{18}O$ for N_2O mixing ratios above or below 200 ppbv for the different data sets and individual ER-2 deployments were also observed (see Table 1 for a summary of ε_{app} values).

[34] As discussed in section 2, the ratios of enrichment factors have been suggested as a means to investigate the possible contribution of the $O(^1D)$ sink to observed changes in the isotope:N_2O relationships since transport should have a minimal effect on the ratios [*Röckmann et al.*, 2001; *Kaiser et al.*, 2002a]. In previous publications, the ratios of enrichment factors were derived by separating the individual data sets into two groups ($N_2O > 200$ ppbv or $N_2O < 200$ ppbv [*Röckmann et al.*, 2001] or altitude <24 km or >24 km [*Toyoda et al.*, 2001]), deriving individual ε values by fitting a line to the data in Rayleigh format, and then taking the quotient of the values to obtain the ratio of interest. For this study, we simply plot the observations as $\ln(\delta^y/1000 + 1) - \ln(\delta^y_o/1000 + 1)$ versus $\ln(\delta^x/1000 + 1) - \ln(\delta^x_o/1000 + 1)$, where δ^x_o and δ^y_o are the tropospheric values (i.e., the values entering the stratosphere) [*Park et al.*, 2002; see also *Kaiser*, 2002]. In this case, the slope of the plotted relationship corresponds to $\varepsilon_{app}(y)/\varepsilon_{app}(x)$ directly,

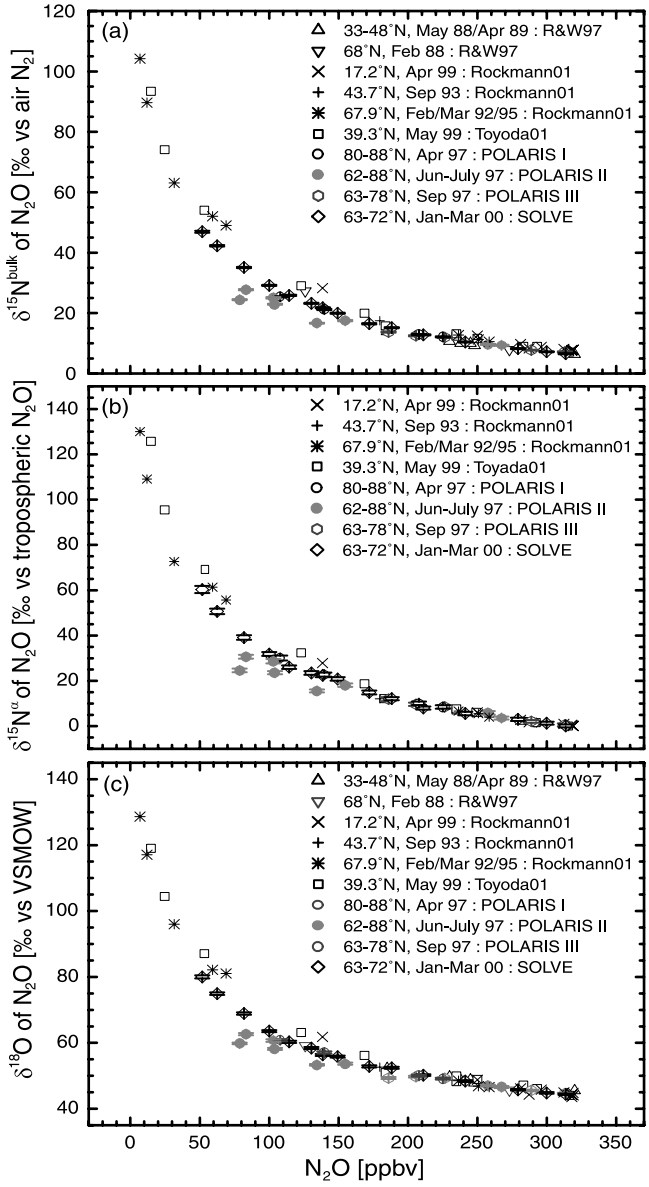

Figure 1. (a) Measurements of $\delta^{15}N^{bulk}$ (‰ versus air-N_2) versus N_2O mixing ratio (ppbv). Uncertainties ($\pm 1\sigma$) for the ER-2 measurements are indicated by the horizontal bars. (b) $\delta^{15}N^{\alpha}$ (‰ versus tropospheric N_2O) versus N_2O mixing ratio, and (c) $\delta^{18}O$ (‰ versus VSMOW) versus N_2O mixing ratio. Here, R&W97, *Rahn and Wahlen* [1997]; Rockmann01, *Röckmann et al.* [2001]; Toyoda01, *Toyoda et al.* [2001].

thus providing a more continuous and less arbitrary picture of how the ratio of enrichment factors for the different isotopologues change with N_2O mixing ratio and allowing visual inspection of the data to see which data points may be outliers. It also means that any small measurement offsets in tropospheric N_2O isotopic compositions based on slightly different laboratory isotope scales are accounted for. The observations for $\delta^{15}N^{\alpha}$ and $\delta^{15}N^{bulk}$ are plotted as $\ln(\delta^{15}N^{\alpha}/1000 + 1) - \ln(\delta^{15}N_o^{\alpha}/1000 + 1)$ versus $\ln(\delta^{15}N^{bulk}/1000 + 1) - \ln(\delta^{15}N_o^{bulk}/1000 + 1)$ for the ER-2 measurements and for the *Röckmann et al.* [2001] and *Toyoda et al.* [2001] balloon data in Figure 3a (all observations) and 3b (observations for $N_2O > 200$ ppbv). For reference, the experimentally determined ratios of enrichment factors, or $\varepsilon(^{15}N^{\alpha})/\varepsilon(^{15}N^{bulk})$, for photolysis [*Röckmann et al.*, 2001] and for reaction with $O(^1D)$ [*Kaiser et al.*, 2002a] are also plotted. The values of the ratios (i.e., the slopes) and their uncertainties were calculated using an ordinary linear least squares regression, a robust MM regression, a geometric mean regression (which accounts for errors in both the x and y variables and is the method of choice for small data sets (*Ricker* [1973]; see also *Miller and Tans* [2003] for a recent discussion)), and a weighted least-squares regression (which accounts for errors of different magnitudes in both the x and y variables [*Williamson*, 1968]). In the following discussion and figures, the geometric mean regression results (and their 2σ uncertainties) are always stated, although in each case the statistical conclusions are the same regardless of regression method used. We also performed statistical t-tests; the confidence to which we can state that two measured values are the same are in this case likewise given by the errors and/or the equivalent confidence intervals stated (i.e., 1.96σ corresponds to a 95% confidence interval, 2.58σ to a 99% confidence interval, etc.).

[35] From Figures 3a and 3b, we note the following. First, the observed ratio $\varepsilon(^{15}N^{\alpha})/\varepsilon(^{15}N^{bulk})$ appears to vary little between different data sets and different ER-2 deployments, even though the enrichment factors were quite different for data corresponding to $N_2O < 200$ ppbv (compare Figure 2). Second, the value for the ratio $\varepsilon(^{15}N^{\alpha})/\varepsilon(^{15}N^{bulk})$ derived from a geometric mean regression of all the combined stratospheric observations is 1.38 ± 0.01 (2σ), a value not statistically different from 1.39 ± 0.07, which is the ratio obtained from all the data points with N_2O mixing ratios >200 ppbv, or from 1.36 ± 0.02, which is the ratio obtained for $N_2O < 200$ ppbv. Therefore a change in the enrichment

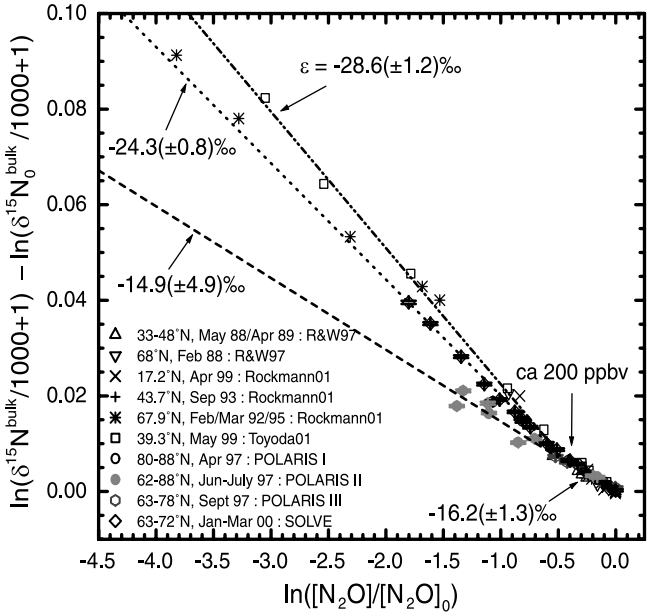

Figure 2. Rayleigh plot for $\delta^{15}N^{bulk}$ of N_2O. The lines are linear regression fits and the slopes yield the apparent enrichment factors. All data points for N_2O mixing ratios > 200 ppbv fall on a line with $\varepsilon_{app}(^{15}N^{bulk}) = -16.2 \pm 1.3$ (2σ) ‰.

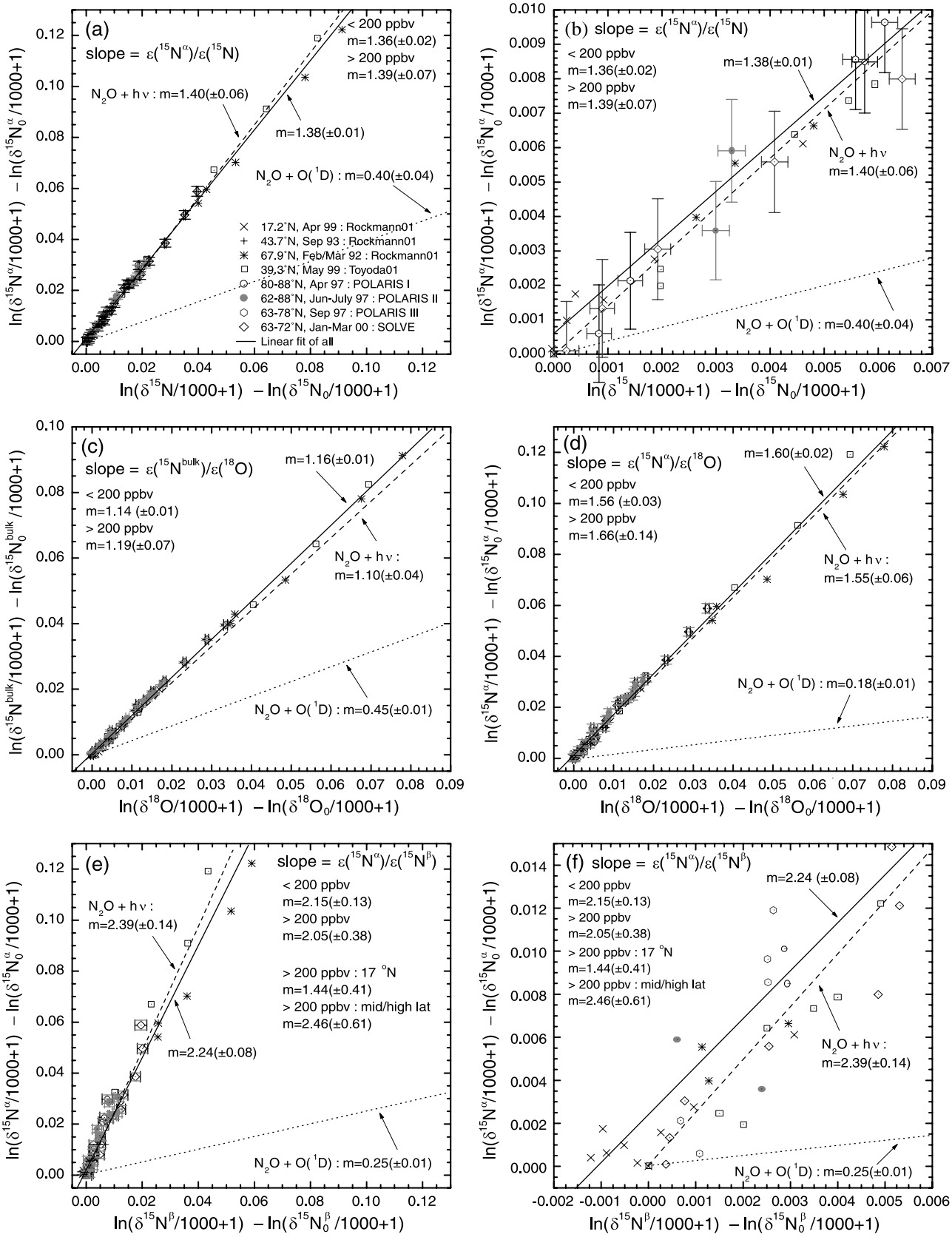
(a)
slope = ε(15Nα)/ε(15N)
< 200 ppbv
m=1.36(±0.02)
> 200 ppbv
m=1.39(±0.07)
N2O + hν : m=1.40(±0.06)
m=1.38(±0.01)
N2O + O(1D) : m=0.40(±0.04)
17.2°N, Apr 99 : Rockmann01
43.7°N, Sep 93 : Rockmann01
67.9°N, Feb/Mar 92 : Rockmann01
39.3°N, May 99 : Toyoda01
80-88°N, Apr 97 : POLARIS I
62-88°N, Jun-July 97 : POLARIS II
63-78°N, Sep 97 : POLARIS III
63-72°N, Jan-Mar 00 : SOLVE
Linear fit of all
ln(δ15Nα/1000+1) − ln(δ15Nα0/1000+1)
ln(δ15N/1000+1) − ln(δ15N0/1000+1)
(b) slope = ε(15Nα)/ε(15N)
< 200 ppbv
m=1.36(±0.02)
> 200 ppbv
m=1.39(±0.07)
m=1.38(±0.01)
N2O + hν
m=1.40(±0.06)
N2O + O(1D) : m=0.40(±0.04)
(c)
slope = ε(15Nbulk)/ε(18O)
< 200 ppbv
m=1.14 (±0.01)
> 200 ppbv
m=1.19(±0.07)
m=1.16(±0.01)
N2O + hν :
m=1.10(±0.04)
N2O + O(1D) : m=0.45(±0.01)
ln(δ15Nbulk/1000+1) − ln(δ15Nbulk0/1000+1)
ln(δ18O/1000+1) − ln(δ18O0/1000+1)
(d)
slope = ε(15Nα)/ε(18O)
< 200 ppbv
m=1.56 (±0.03)
> 200 ppbv
m=1.66(±0.14)
m=1.60(±0.02)
N2O + hν :
m=1.55(±0.06)
N2O + O(1D) : m=0.18(±0.01)
(e)
slope = ε(15Nα)/ε(15Nβ)
N2O + hν :
m=2.39(±0.14)
< 200 ppbv
m=2.15(±0.13)
> 200 ppbv
m=2.05(±0.38)
> 200 ppbv : 17 °N
m=1.44(±0.41)
> 200 ppbv : mid/high lat
m=2.46(±0.61)
m=2.24(±0.08)
N2O + O(1D) : m=0.25(±0.01)
ln(δ15Nβ/1000+1) − ln(δ15Nβ0/1000+1)
(f) slope = ε(15Nα)/ε(15Nβ)
< 200 ppbv
m=2.15(±0.13)
> 200 ppbv
m=2.05(±0.38)
> 200 ppbv : 17 °N
m=1.44(±0.41)
> 200 ppbv : mid/high lat
m=2.46(±0.61)
m=2.24 (±0.08)
N2O + hν :
m=2.39(±0.14)
N2O + O(1D) : m=0.25(±0.01)

factor ratios, $\varepsilon(^{15}N^{\alpha})/\varepsilon(^{15}N^{bulk})$ between low and high N_2O mixing ratios cannot be distinguished above the measurement uncertainties. Third, the values for the ratio $\varepsilon(^{15}N^{\alpha})/\varepsilon(^{15}N^{bulk})$ of 1.38 ± 0.01, 1.39 ± 0.07, and 1.36 ± 0.02 derived from all the observations for all N_2O, for N_2O > 200 ppbv, and for N_2O < 200 ppbv appear to be primarily explained by the experimental value of 1.40 ± 0.06 for photolysis over relevant stratospheric wavelengths [*Röckmann et al.*, 2001] or a slope of 1.30 ± 0.06 assuming a global 9:1 ratio of experimental values for photolysis [*Röckmann et al.*, 2001] and reaction with $O(^1D)$ [*Kaiser et al.*, 2002a].

[36] Similar results are observed for $\varepsilon(^{15}N^{bulk})/\varepsilon(^{18}O)$, $\varepsilon(^{15}N^{\alpha})/\varepsilon(^{18}O)$, and $\varepsilon(^{15}N^{\alpha})/\varepsilon(^{15}N^{\beta})$, shown in Figures 3c–3f. For $\varepsilon(^{15}N^{bulk})/\varepsilon(^{18}O)$ and $\varepsilon(^{15}N^{\alpha})/\varepsilon(^{18}O)$ in Figures 3c and 3d, respectively, the slope derived from all the observations is statistically the same as those derived for N_2O > 200 ppbv and N_2O < 200 ppbv, and are well described by the ratio derived from the photolysis experiments or from a 9:1 global ratio between the experimental photolysis and $O(^1D)$ oxidation data. The observations for $\varepsilon(^{15}N^{\alpha})/\varepsilon(^{15}N^{\beta})$ in Figures 3e and 3f deserve special attention. While the ER-2 and *Toyoda et al.* [2001] balloon data appear to follow the experimental photolysis line, the 3 lowest N_2O observations from the *Röckmann et al.* [2001] balloon data fall below that line. Even with these 3 points, however, the slope of the line for the combined observations is still within the 2σ limit for agreement with the experimental photolysis data (i.e., 2.24 ± 0.08 versus 2.39 ± 0.14) or with a 9:1 global ratio between the experimental photolysis and $O(^1D)$ oxidation data (i.e., 2.24 ± 0.08 versus 2.18 ± 0.13). Furthermore, the slopes of the relationships for all N_2O, for N_2O > 200 ppbv, and for N_2O < 200 ppbv all agree within their 2σ limits. If the Röckmann et al. balloon data are removed and only the ER-2 and Toyoda et al. balloon data are included, the $\varepsilon(^{15}N^{\alpha})/\varepsilon(^{15}N^{\beta})$ ratios are 2.65 ± 0.10, 2.50 ± 0.78, and 2.58 ± 0.15 for all N_2O, N_2O > 200 ppbv, and N_2O < 200 ppbv, respectively, in even closer agreement. Even the Toyoda et al. data set alone yields $\varepsilon(^{15}N^{\alpha})/\varepsilon(^{15}N^{\beta})$ ratios for all N_2O, N_2O < 200 ppbv, and N_2O > 200 ppbv that are within 1σ agreement (see Table 1 for the published *Toyoda et al.* [2001] ratios; values from our geometric mean regression analysis of their data are 2.70 ± 0.69 and 2.63 ± 0.19 for N_2O > 200 ppbv and N_2O < 200 ppbv, respectively). In contrast, while the slopes for the Röckmann et al. data alone for N_2O > 200 ppbv and N_2O < 200 ppbv are just within their 2σ limits of each other (see section 2), a reanalysis of the Röckmann et al. data by *Kaiser* [2002], using a "continuous" method similar to that used here but with a least squares regression and including a data point at 179.7 ppbv N_2O along with the N_2O > 200 ppbv points, places the ratios just outside their 2σ limits (1.5 ± 0.2 for N_2O > 179 ppbv and 2.0 ± 0.2 for N_2O < 140 ppbv). Our own least squares and geometric mean analyses of their data show that there is a difference between the $\varepsilon(^{15}N^{\alpha})/\varepsilon(^{15}N^{\beta})$ ratios at the 2σ level when the data point at N_2O = 179.7 ppbv is included with the high-N_2O data (although not for N_2O > 200 ppbv). Thus there does appear to be a statistically significant difference at the 2σ level at high and low N_2O values in the Röckmann et al. data set.

[37] Since the difference in values for the ratio $\varepsilon(^{15}N^{\alpha})/\varepsilon(^{15}N^{\beta})$ between high and low N_2O mixing ratios in the *Röckmann et al.* [2001] data set has been interpreted as possible evidence for a difference in the relative $O(^1D)$ contribution to the fractionation of the isotopologues in different regions of the stratosphere [e.g., *Kaiser et al.*, 2002a], it is important to investigate why the ER-2 data (obtained in the lower stratosphere where the in situ $O(^1D)$ contribution to N_2O destruction is the largest) do not show a difference in the $\varepsilon(^{15}N^{\alpha})/\varepsilon(^{15}N^{\beta})$ values. An additional means of binning the observations may provide new insight. In addition to N_2O mixing ratios, the combined data set can be divided up into measurements on subtropical air (the Röckmann et al. data at 17°N) versus air characteristic of middle and high latitudes (Note that in the lower and middle stratosphere, long-lived tracer:tracer correlations measured in situ from the ER-2 and balloons show that there are distinct differences between the tropics and midlatitudes and that 17°N is clearly in a transition region between the two [e.g., *Murphy et al.*, 1993; *Jost et al.*, 1998; *Andrews et al.*, 1999]; we therefore consider samples collected at 17°N to be subtropical in character for the analysis here). For this additional binning, the value of $\varepsilon(^{15}N^{\alpha})/\varepsilon(^{15}N^{\beta})$ for N_2O mixing ratios > 200 ppbv is 1.44 ± 0.41 for subtropical air versus 2.46 ± 0.61 for midlatitude and high-latitude air, a difference which is statistically significant at the 2σ level. If this difference in values for $\varepsilon(^{15}N^{\alpha})/\varepsilon(^{15}N^{\beta})$, which are not seen for any other ε/ε ratios, is truly due to atmospheric variability and not to measurement differences between the laboratories, larger relative experimental uncertainties for the higher-N_2O data points, and/or simply too few data points, then it may be due to differences between tropical/subtropical air and older air at higher latitudes rather than differences at high and low N_2O mixing ratios since the high-N_2O data of Röckmann et al. is dominated by the balloon flight at 17°N (6 out of 9 measurements for N_2O > 200 ppbv, or 6 out of 10 for the reanalysis by *Kaiser* [2002]). The potential significance of the observations and analysis presented here is discussed further below.

5. Discussion

[38] The implications of the observations for the effects of stratospheric transport and chemistry on the N_2O isotope compositions are discussed in sections 5.1 and 5.2 below. In

Figure 3. (a) Slope of the solid line derived from the scatterplot, representing the ratio of enrichment factors $\varepsilon(^{15}N^{\alpha})/\varepsilon(^{15}N^{bulk})$ for all stratospheric data sets. For reference, the experimentally determined ratios from photolysis [*Röckmann et al.*, 2001] and from reaction with $O(^1D)$ [*Kaiser et al.*, 2002a] are plotted as dashed and dotted lines, respectively. Symbols are the same as in previous figures. (b) Same as Figure 3a but for N_2O > 200 ppbv. (c) The ratio of enrichment factors $\varepsilon(^{15}N^{bulk})/\varepsilon(^{18}O)$ for all data sets. (d) Ratio of enrichment factors $\varepsilon(^{15}N^{\alpha})/\varepsilon(^{18}O)$ for all data sets. (e) The ratio of enrichment factors $\varepsilon(^{15}N^{\alpha})/\varepsilon(^{15}N^{\beta})$ for all data sets. (f) Same as Figure 3e but for N_2O > 200 ppbv only. All values shown in text in Figure 3 are from a geometric mean regression (see text).

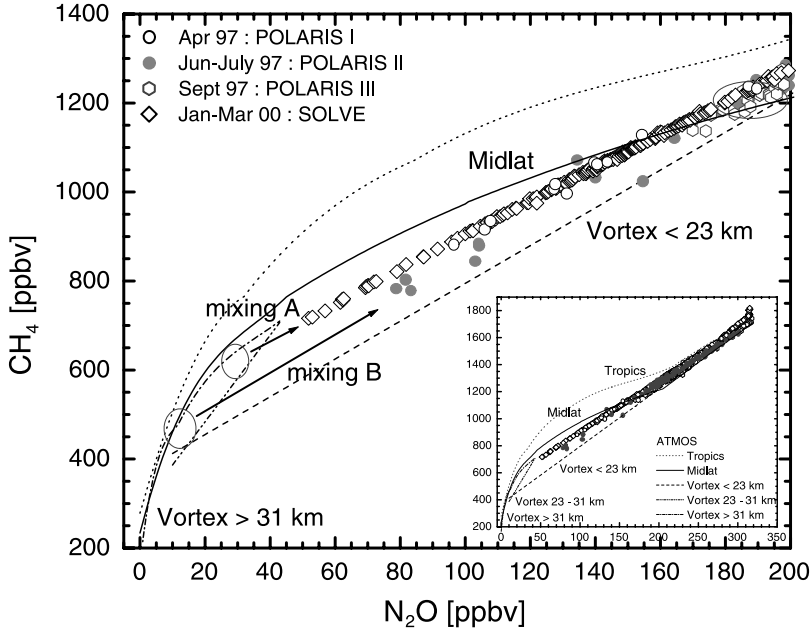

Figure 4. Scatterplot of CH_4 versus N_2O mixing ratios measured from the ER-2 aircraft for N_2O mixing ratios less than ~200 ppbv (the insert shows the plot for the entire range of N_2O). For reference, ATMOS observations of CH_4:N_2O relationships in the tropics, midlatitudes, and vortex [*Michelsen et al.*, 1998] are plotted as dotted, solid, and dashed/dash-dotted lines. Solid black circles denote mixing between two end-member air masses from *Rex et al.* [1999], and the arrows illustrate mixing lines.

section 5.3, we discuss several means of estimating the fluxes of the heavy N_2O isotopologues from the lower stratosphere to the troposphere from stratospheric observations, provide these fluxes, and discuss the associated uncertainties in the context of the global isotope budget for N_2O.

5.1. Influence of Transport and Mixing on Isotopic Compositions

[39] The isotope:N_2O relationships measured from the ER-2 aircraft during the POLARIS II deployment are significantly different (at the 3.29σ level) from those measured during the POLARIS I and SOLVE campaigns and from other observations for N_2O mixing ratios less than 200 ppbv (Figures 1 and 2). An independent analysis of in situ and remote observations of CH_4 and N_2O mixing ratios from balloon and aircraft platforms by *Rex et al.* [1999] showed that vortex filaments encountered during POLARIS I and POLARIS II (i.e., the data points with $N_2O < 200$ ppbv for the isotope data set presented here) were a mixture of high-N_2O and low-N_2O end-members and that the low N_2O end-members were different for the two deployments. Thus the difference in the CH_4:N_2O mixing ratio (as well as other tracer) relationships between POLARIS I and POLARIS II is explained entirely by transport and mixing. We show here that the observed differences in the N_2O isotope:N_2O mixing ratio relationships between POLARIS I/SOLVE and POLARIS II whole air samples are entirely consistent with the transport-only CH_4:N_2O mixing ratio analysis of *Rex et al.* [1999] and that this leaves little room for isotope chemistry to play a role.

[40] First, we examine simultaneous measurements of CH_4 and N_2O mixing ratios from the ER-2 deployments and compare them with remote observations from the ATMOS instrument on board the Space Shuttle [*Michelsen et al.*, 1998]. The ATMOS measurements show compact and distinct correlations between CH_4 and N_2O mixing ratios for tropical, midlatitude, and vortex air (represented by solid and dashed lines in Figure 4). The relationship between CH_4 and N_2O in the tropics and midlatitudes is curvilinear while the relationship in vortex air is typically linear at lower altitudes. The linear vortex relationship for altitudes below 23 km is the result of mixing of higher-altitude, low-N_2O midlatitude air (from which the vortex forms at the beginning of winter) with extra-vortex (i.e., midlatitude) air during or after descent [*Michelsen et al.*, 1998; see also *Kondo et al.*, 1999; *Herman et al.*, 1998; *Waugh et al.*, 1997]. The mixing of higher-altitude, low-N_2O vortex air with lower altitude, high-N_2O air results in an observed CH_4:N_2O relationship that follows a mixing line between the two characteristic air masses. While the ATMOS observations were made in the vortex, measurements of CH_4 and N_2O from the ER-2 aircraft from a number of different aircraft missions have shown that these same mixing line relationships can also be detected in filaments of vortex air which can remain in the atmosphere for some time after the break-up of the vortex in spring [e.g., *Waugh et al.*, 1997; *Michelsen et al.*, 1999].

[41] For the POLARIS and SOLVE ER-2 deployments, the measured CH_4:N_2O correlations are also linear (symbols in Figure 4) and are therefore consistent with measurements in vortex air, remnants of vortex air, or a mixture of vortex and extravortex air. Note that there are small but significant differences between the CH_4:N_2O correlation for the POLARIS II versus the POLARIS I/SOLVE data for $CH_4 < 1200$ ppbv and $N_2O < 180$ ppbv (Figure 4). In their analysis of in situ CH_4 and N_2O measurements from the

ER-2 and balloon platforms made during the POLARIS campaign noted above, *Rex et al.* [1999] showed that the POLARIS I data are consistent with vortex air which is a mixture of air with an N_2O mixing ratio of ~200 ppbv (characteristic of altitudes of ~20 km) with air with an N_2O mixing ratio of ~25 to 40 ppbv (characteristic of altitudes of ~32 to 34 km). Such a mixture is denoted in Figure 4 as mixing line A. The analysis by *Rex et al.* [1999] also showed that filaments of vortex air were sampled in northern summer during the POLARIS II deployment [see also *Newman et al.*, 1999]. The vortex filaments remained measurable several months after the break-up of the polar vortex because of weak transport at high latitudes in the summer [e.g., *Newman et al.*, 1999]. These filaments from POLARIS II were determined to be a mixture of even lower N_2O air which had originated from higher up in the vortex (with ~15 to 20 ppbv N_2O, characteristic of altitudes of ~37 km) with air with an N_2O mixing ratio of ~200 ppbv N_2O. Such a mixture is denoted in Figure 4 as mixing line B. Whether this isentropic mixing across the vortex edge occurs throughout the winter ("continuous weak mixing") or after the period of rapid descent (i.e., March or later, "late end-member mixing") is still under debate [see, e.g., *Plumb et al.*, 2000; *Rex et al.*, 1999]. In either case, however, the observed CH_4:N_2O correlation was different between the POLARIS I and II deployments due solely to mixing processes occurring in or near the vortex.

[42] Since the difference in the CH_4:N_2O mixing ratio relationships between the POLARIS II and the POLARIS I/SOLVE observations is due to transport and not chemistry, the two mixing scenarios denoted A and B in Figure 4 can be applied to the isotope:N_2O relationships to check for consistency. Mixing lines for isotope ratios are not as intuitively obvious as those for mixing ratio relationships, however. Rather than forming simple mixing lines between mixing ratios as in Figure 4, the results of mixing on an isotope:N_2O plot are curves that lie below the isotope:N_2O relationship since the mixing causes the N_2O isotopic composition to be lighter for a given N_2O mixing ratio. If the mixing process can be represented as two-end-member mixing, equation (6) [e.g., *Criss*, 1999] can be used to relate the resulting N_2O isotopic compositions and mixing ratios

$$R = \frac{R_1 m_1 F_1 + R_2 m_2 F_2}{m_1 F_1 + m_2 F_2} \quad (6)$$

where R represents the resulting isotope ratio of interest after mixing, m_1 and m_2 are the N_2O mixing ratios for the two end-members, and F_1 and F_2 are the fractions of the total volume of air mixed together that each end-member contributed.

[43] Since few observations are available for the isotopic compositions of high-altitude midlatitude air at N_2O mixing ratios of 15 to 40 ppbv (i.e., those indicated by the CH_4:N_2O tracer analysis for the high-altitude end-members for the vortex and vortex filament air), we first use equation (6) to estimate what the low-N_2O-mixing-ratio end-members might be and whether the difference in the isotope:N_2O relationships between POLARIS I/SOLVE and POLARIS II due to mixing can be at least qualitatively simulated in a way that is consistent with the mixing inferred from the CH_4:N_2O tracer relationships. In Figure 5, mixing line A is simulated

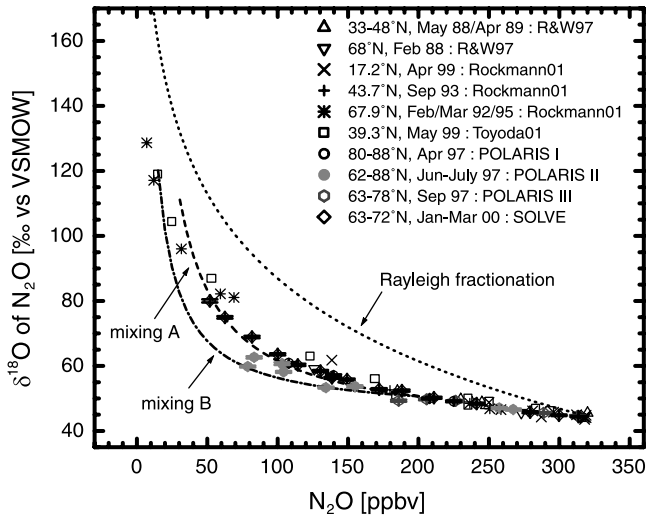

Figure 5. The $\delta^{18}O$ of N_2O (‰ versus VSMOW) versus N_2O mixing ratio, along with the Rayleigh fractionation curve derived from the UV broadband photolysis experiment [*Röckmann et al.*, 2001]. The two lower dashed lines illustrate the resulting $\delta^{18}O$:N_2O correlations from a two-end-member mixing model for the two different mixing scenarios discussed for Figure 4.

to approximate the POLARIS I/SOLVE $\delta^{18}O$:N_2O relationship, with N_2O = 30 ppbv and $\delta^{18}O$ = 112.2‰ for end-member 1 and N_2O = 200 ppbv and $\delta^{18}O$ = 50.7‰ for end-member 2. Mixing line B is simulated to approximate the POLARIS II $\delta^{18}O$:N_2O relationship, with N_2O = 15 ppbv and $\delta^{18}O$ = 120.5‰ for end-member 1 and N_2O = 200 ppbv and $\delta^{18}O$ = 50.7‰ for end-member 2. Thus this simple mixing scenario to reproduce the isotope:N_2O relationships due to mixing of air at different altitudes in the vortex is indeed consistent with the mixing origin of the simultaneous CH_4:N_2O tracer relationships observed for POLARIS I/SOLVE and POLARIS II deployments by *Rex et al.* [1999]. Moreover, we also note that this mixing-only origin is also consistent with simultaneous measurements of the CH_4 isotope:CH_4 mixing ratio relationships between POLARIS II and POLARIS I/SOLVE samples as well [*McCarthy et al.*, 2003].

[44] A more quantitative analysis can be pursued once more isotope ratios in high-altitude midlatitude air at N_2O mixing ratios from 10 to 40 ppbv are measured. Nonvortex midlatitude to high-latitude data obtained at the time of or just before the formation of the vortex is needed to provide the initial end-members, since these data would represent the "initial conditions" for air inside the vortex. Until these measurements are available, it is not clear whether or not the *Röckmann et al.* [2001] balloon data (taken in the vortex in February/March 1992) or the *Toyoda et al.* [2001] balloon data (taken in May 1999, which could be influenced by the break-up of the vortex or vortex remnants) are representative of the initial conditions in the vortex. When data are available, it may be possible to use the isotope:N_2O relationships from POLARIS, SOLVE and future missions to explore whether isentropic mixing across the vortex edge is accomplished by late end-member mixing or by continuous weak mixing throughout the winter since continuous

weak mixing should depart from the behavior given by equation (6) and follow a mathematically different (and more complex) relationship (K. A. Boering et al., manuscript in preparation, 2003). In either case, however, the underlying cause for the low values for ε_{app} observed for all the N_2O isotopologues during POLARIS II can be explained by mixing and transport; any additional effects of isotope chemistry on the ε_{app} values must in this case be small to negligible.

[45] In general, transport and mixing also explain a large part of the small but discernable differences between the isotope:N_2O relationships observed in subtropical air (17.2°N [*Röckmann et al.*, 2001]), midlatitude air (39.3°N [*Toyoda et al.*, 2001]), and high-latitude air (63–88°N; POLARIS I/SOLVE and *Röckmann et al.* [2001]). In Figure 5, for example, the values for $\delta^{18}O$ of N_2O are in general lighter for a given N_2O mixing ratio upon moving from subtropical air to middle to high latitudes, and all are lighter than that predicted from the Rayleigh fractionation curve for photolysis in an isolated system. (Note that some of the variability in the high-latitude Röckmann et al. data is likely due to sampling vortex and nonvortex air in the single balloon profile.) This increasing attenuation of the underlying isotope effects as a function of latitude is at least in part due to the fact that the subtropics are relatively more isolated and less influenced by transport and mixing compared with the midlatitudes, and likewise for a comparison of midlatitude air with vortex air at high latitudes. This dependence on latitude, for example, is observed and successfully modeled for the CH_4 isotope:CH_4 mixing ratio relationships, even though the oxidant-weighted ε values themselves are actually smaller in the tropics than the extratropics because of the increased fraction of CH_4 oxidation by $O(^1D)$ in the tropics relative to OH and Cl, which have larger individual ε values than $O(^1D)$ (*McCarthy et al.* [2003]; see also *Rice et al.* [2003, and references therein] for the relative isolation of the tropics compared with the extratropics in general). Thus, at least for CH_4 isotopologues, transport and mixing are entirely responsible for the decrease in ε_{app} values with increasing latitude. For N_2O, it remains to be seen how much chemistry could also play a role beyond transport in the differences in ε_{app} values with latitude; additional N_2O isotope data in the tropics and comparisons with model results should help address this question.

5.2. Comparison of ε_{app} and ε/ε Values As a Function of N_2O

[46] As discussed in section 2, the apparent isotopic enrichment factors, ε_{app}, from balloon observations have been shown to change significantly for N_2O mixing ratios above or below 200 ppbv [*Röckmann et al.*, 2001] or, approximately equivalently for balloon profiles, altitudes above or below 24 km [*Toyoda et al.*, 2001]. With the addition of the new ER-2 data to the stratospheric N_2O isotope database, we see that the variations in ε values are as large for $N_2O < 200$ ppbv between the POLARIS II and POLARIS I/SOLVE deployments (−14.9 to −24.3‰, respectively, for $\varepsilon(^{15}N^{bulk})$) as the difference between ε values for the combined stratospheric database for $N_2O > 200$ ppbv and the ER-2 SOLVE observations for $N_2O < 200$ ppbv (−16.2 to −24.3‰, respectively, for $\varepsilon(^{15}N^{bulk})$). Since the differences between the POLARIS II and the POLARIS I/SOLVE enrichment factors can be explained by mixing and transport alone, it is not unreasonable to expect that the differences in values for ε_{app} for the balloon data for $N_2O < 200$ ppbv and $N_2O > 200$ ppbv may also result from transport and mixing alone.

[47] As discussed in section 2, however, isotope chemistry may also contribute to these differences in ε_{app} values as a function of N_2O mixing ratio, and *Röckmann et al.* [2001] and *Kaiser et al.* [2002a] proposed investigating the ratios of ε values for the different isotopologues as a means to effectively normalize the ε_{app} values for the effects of transport and, with transport effects cancelled out, to potentially distinguish the relative contributions of $O(^1D)$ versus photolysis to the overall N_2O destruction rate [e.g., *Kaiser et al.*, 2002a]. Although large differences in the value for ε_{app} observed for POLARIS II for $N_2O < 200$ ppbv with respect to all other balloon and ER-2 data for $N_2O < 200$ ppbv were observed, the ratios of ε values for $\varepsilon(^{15}N^{\alpha})/\varepsilon(^{15}N^{bulk})$, $\varepsilon(^{15}N^{bulk})/\varepsilon(^{18}O)$, and $\varepsilon(^{15}N^{\alpha})/\varepsilon(^{18}O)$ for the ER-2 data are the same to within their 1σ limits (see Table 1). For $\varepsilon(^{15}N^{\alpha})/\varepsilon(^{15}N^{\beta})$, the ER-2 data for $N_2O < 200$ ppbv for the POLARIS II versus POLARIS I/SOLVE measurements agree to within their 2σ uncertainty but not within their 1σ uncertainty. If these ratios are truly different and not just a result of too few measurements from POLARIS II, it is unlikely that this lower average value for the POLARIS II vortex remnant observations could be due to an increase in the relative proportion of N_2O loss by $O(^1D)$ over the oxidation and photolysis history of the air masses measured. Rather, if these differences are real, perhaps transport does not entirely cancel out for the mixing conditions near the vortex barrier (for POLARIS II) or, by analogy, near the subtropical barrier (for the Röckmann et al. data). If these differences are found to not be statistically significant, however, (e.g., when more data are available) then the simplest explanation of the ER-2 data and of the combined ER-2 and balloon data is that no difference in the contribution from $O(^1D)$ for the lower altitude data/higher-N_2O observations can be discerned from that for the higher-altitude/lower N_2O observations. If this is true, it is not surprising. Although the contribution of $O(^1D)$ to the in situ N_2O destruction rate in the lower stratosphere may be as large as 14%, the lifetime of N_2O below altitudes of 22 km is longer than 100 years (on the basis of Lawrence Livermore National Laboratory 2-D model calculations done at UC Berkeley). Hence N_2O mixing ratios below the tropospheric value of ~315 ppbv measured in the lower stratosphere are predominantly the result of destruction higher up in the stratosphere at 25 to 35 km between 30°S and 30°N [*Minschwaner et al.*, 1993] and subsequent transport to lower altitudes rather than by in situ photochemistry.

[48] Alternatively, as explored in section 4, there may indeed be a difference in the values for $\varepsilon(^{15}N^{\alpha})/\varepsilon(^{15}N^{\beta})$ measured in subtropical air by *Röckmann et al.* [2001] and analyzed here that would be worth pursuing further with additional observations for confirmation. As noted in section 4, the value for $\varepsilon(^{15}N^{\alpha})/\varepsilon(^{15}N^{\beta})$ for $N_2O > 200$ ppbv in subtropical air (which corresponds to altitudes <24 km) is statistically different at the 2σ level from the combined stratospheric data set for $N_2O > 200$ ppbv at middle to high latitudes (1.44 ± 0.41 versus 2.46 ± 0.61, respectively; see

Figures 3e and 3f). Yet, given the argument above that the lifetime of N_2O is quite long at 24 km and below, it is not clear whether a smaller value for $\varepsilon(^{15}N^{\alpha})/\varepsilon(^{15}N^{\beta})$ due to an increase in the relative contribution of $O(^1D)$ to N_2O destruction there could be detectable or not. Additional data should help distinguish all the possibilities discussed here, particularly since the values for $\varepsilon(^{15}N^{\alpha})/\varepsilon(^{15}N^{\beta})$ for the Röckmann et al. data set and for the POLARIS II observations depend sensitively on only several data points out of the total number of stratospheric observations from the ER-2 data set (32), the balloon data set (16), and the *Toyoda et al.* [2001] data set (11). For now, we conclude that the addition of the ER-2 data to the Röckmann et al. and Toyoda et al. balloon data sets does not add statistical weight to possible differences in $\varepsilon(^{15}N^{\alpha})/\varepsilon(^{15}N^{\beta})$ values in the lower versus middle regions of the stratosphere but that differences between the subtropical and extratropical air cannot be ruled out.

5.3. Fluxes of N_2O Isotopologues From the Stratosphere to the Troposphere

[49] The ER-2 observations, combined with earlier aircraft and balloon measurements, show that the isotopologue:N_2O relationships, and therefore the enrichment factors, are remarkably constant in the lower stratosphere for N_2O mixing ratios >200 ppbv, regardless of the wide range of years, seasons, and locations in which samples were collected. Since the lower stratosphere is the source region for air returning to the troposphere, we can with confidence use the ER-2 observations to calculate the fluxes of enriched isotopologues from the stratosphere to the troposphere. As explained below, the fluxes, or more specifically, the isotope fluxes (sometimes referred to as ''isofluxes'' by biogeochemists) defined below, can be determined to within an uncertainty of ±25%. This level of uncertainty is considerably smaller than those for the isotope-weighted N_2O emissions [e.g., *Bouwman et al.*, 1995; *Prather and Ehhalt*, 2001].

[50] In Appendix A we derive several sets of equations used to estimate the net annual fluxes of the N_2O isotopologues from the stratosphere to the troposphere with both exact and approximate expressions in the various (and differing) traditions of isotope biogeochemists (who favor box models) and stratospheric chemists (who favor tracer:tracer relationships or 2-D and 3-D computer simulations). While two recent studies have also used box model approaches to investigate the influence of stratospheric fractionation on N_2O isotope compositions in the free troposphere [*Rahn and Wahlen*, 2000; *Röckmann et al.*, 2003a], our main goal here is to show explicitly that some of the uncertainties in the isotope flux estimates, such as the mass flux of air between the stratosphere and troposphere that Rahn and Wahlen were concerned with and avoided in their one-box model formulation, do not result in unreliable fluxes. Rather, as we will show, the main uncertainty for all approaches is the global N_2O loss rate. A second goal is to show that the various approaches found in the literature for estimating isotope fluxes, including the recent 3-D CTM modeling study of *McLinden et al.* [2003] and use of the so-called ''Plumb and Ko relationship'' for long-lived tracers in the stratosphere [e.g., *Luz et al.*, 1999], are approximately equivalent to within several approximations. Finally, the third goal is to provide explicit isotope fluxes for all the heavy N_2O isotopologues and their uncertainties that future modelers can use in their analyses of the global N_2O isotope budget. While details appear in Appendix A, we give a brief description of our approach here and the results.

[51] First, we note that the net isotope flux can be derived phenomenologically from the slope of the correlation of the isotopologue with a long-lived tracer whose vertical flux is known. This type of approach has been used by stratospheric chemists to estimate the net flux of NO_y [*Murphy and Fahey*, 1994; *McLinden et al.*, 2000], O_3 [*Murphy and Fahey*, 1994; *McLinden et al.*, 2000; *Olsen et al.*, 2001] and the $^{17}O-^{18}O$ anomaly in CO_2 [*Luz et al.*, 1999] from the stratosphere to the troposphere based on the observed slope of the relationship between N_2O and the species of interest. *Plumb and Ko* [1992] showed that the observed slope between two long-lived tracers is equal to the ratio of the net vertical fluxes of the two species. For N_2O, the net vertical flux is equal to the global loss rate, which has been quantified by a convolution of satellite and balloon observations of N_2O with models of photolysis rates and rates for reaction with $O(^1D)$ [see, e.g., *Minschwaner et al.*, 1993]. The loss rate is thus known to an uncertainty of ±25% (To be more exact, the net vertical flux is equal to the loss rate plus the growth rate of N_2O in the stratosphere; see Appendix A for details). In Appendix A an estimate for the net isotope fluxes of the N_2O isotopologues from the slope of the N_2O isotopologue:N_2O relationship is given by equation (A12).

[52] For comparison, the preferred form of the N_2O isotopologue flux for isotope biogeochemists is the net isotope flux from a box-model approach. Effectively equivalent to a *Plumb and Ko* [1992] approach, this form is essentially the N_2O flux weighted by the change in isotopic composition in the stratosphere (equation (7)).

$$\text{Net isotope flux} = F_{ST}(\delta_S - \delta_T) \tag{7}$$

F_{ST} is the flux of N_2O from the stratosphere to the troposphere and $(\delta_S - \delta_T)$ is the difference between the isotopic composition of the species of interest entering the troposphere and that leaving the troposphere. For the expression (equation (A9)) for the net isotope flux from a box model formation (as well as for the phenomenological Plumb and Ko expression in equation (A12)), annual mean fluxes of air between the stratosphere and troposphere must be used. We use the fluxes calculated from radiative and dynamical considerations by *Holton* [1990] and *Appenzeller et al.* [1996]. These two studies calculated the mass flux of air across the 100-hPa pressure surface and the 380 K isentropic surface and yielded values of 2.0×10^{17} kg yr^{-1} and 6.8×10^{17} kg yr^{-1}, respectively. (Note that the 380 K surface in the extratropics lies approximately between ~100 and 160 hPa depending on season and latitude.) Although values for F_{ST} in equation (7) depend on which stratosphere-troposphere mass flux is used, so do the values for δ_S; the larger mass flux yields a higher mixing ratio for N_2O in air returning to the troposphere, which, in turn yields a smaller value for δ_S for N_2O in air returning to the troposphere (see, e.g., *Luz et al.* [1999], *Röckmann et al.* [2003a], and details in Appendix A). Thus the values for the net isotope flux are very nearly the same (see Table 3 for

Table 3. Estimates of the Net Isotope Fluxes Determined From the ER-2 Observations for $N_2O > 200$ ppbv Using a Photochemical Loss Rate of 13 Tg N yr^{-1}

	$F_{ST}\cdot(\delta_S - \delta_T)$				$-\varepsilon \cdot L$	
	100-hPa Surface (F_{ST} = 48 (±12) Tg N yr^{-1}; m_S = 248 ppbv)[a]		380 K Surface (F_{ST} = 195 (±49) Tg N yr^{-1}; m_S = 295 ppbv)[a]			
	$\delta_S - \delta_T$, ‰	Net Isotope Flux, ‰ Tg N yr^{-1}	$\delta_S - \delta_T$, ‰	Net Isotope Flux, ‰ Tg N yr^{-1}	$\lvert\varepsilon\rvert$ for $N_2O > 200$ ppbv, ‰	Net Isotope Flux, ‰ Tg N yr^{-1}
$^{15}N^{bulk}$	3.6 (±1.0)	172 (±65)	1.0 (±0.3)	188 (±68)	14.9 (±0.5)	192 (±48)
$^{15}N^{\alpha}$	5.5 (±1.6)	262 (±100)	1.5 (±0.4)	287 (±104)	22.5 (±1.2)	290 (±74)
^{18}O	3.3 (±0.9)	159 (±60)	0.9 (±0.2)	174 (±63)	13.3 (±0.5)	172 (±43)

[a]Uncertainty (±1σ) does not include uncertainty in the annual mass flux of air exchanged between the troposphere and stratosphere calculated by *Holton* [1990] (2.0×10^{17} kg yr^{-1}) and *Appenzeller et al.* [1996] (6.8×10^{17} kg yr^{-1}). $F_{ST} \cdot (\delta_S - \delta_T) \cong \varepsilon \cdot (F \cdot m_T - L) \cdot \ln(1 - L/Fm_T)$, where m_T = 314 ppbv (see Appendix A) and L is the photochemical loss rate.

the ER-2 results based on equation (A9) and compare columns 3 and 5 for the net isotope fluxes for the Holton versus Appenzeller et al. air mass fluxes).

[53] Moreover, if equation (A9) is simplified using a Taylor series expansion to remove the dependence on the mass flux of air between the stratosphere and troposphere, as shown in Appendix A, the net isotope flux is equivalent to the apparent fractionation factor, ε, for $N_2O > 200$ ppbv, multiplied by the N_2O loss rate, L (equation (A10)).

$$F_{ST}(\delta_S - \delta_T) \approx -\varepsilon \cdot L \tag{8}$$

The net isotope fluxes calculated from the approximation in equation (8) are also given in Table 3 in column 7 for comparison. All calculations in Table 3 are based on the ER-2 data using L = 13 Tg N yr^{-1} [*Prather and Ehhalt*, 2001], with an estimated uncertainty of ±25%.

[54] The values calculated from the ER-2 observations are also compared with recent 3-D model results from *McLinden et al.* [2003] in Table 4. McLinden et al. called the quantity "$-\varepsilon \cdot L$" the "flux-weighted enrichment factor (FWEF)" but, as shown in Appendix A, these are essentially equivalent to the net isotope fluxes to within the approximations given in Appendix A. There is remarkably good agreement between the estimates based on the ER-2 observations and the fully modeled values. Moreover, it is clear from our analysis that the largest uncertainty in estimating these rates is the global N_2O loss rate. First, the ER-2 data combined with the rest of the stratospheric measurements demonstrate that there is little uncertainty in the relevant ε_{app} values in the lower stratosphere. Second, even a difference in the mass flux of air between the stratosphere and troposphere of a factor of 3 results in differences in net isotope fluxes of only 8%. We therefore conclude that the net isotope fluxes for heavy isotopologues between the stratosphere and troposphere are now considerably better quantified (to ± 25%) than other important terms in the global N_2O isotope budget.

[55] As a simple illustration of the influence of isotope fractionation in the stratosphere on N_2O isotopic compositions in the free troposphere, we use the isotope fluxes derived from the ER-2 data in a steady state box model of the atmosphere. For simplicity, the natural surface source is separated into its oceanic and terrestrial components in the same proportions as estimated in the IPCC report [*Prather and Ehhalt*, 2001]: 67% for terrestrial sources and 33% for the oceanic source. Published observations of $\delta^{15}N$ and $\delta^{18}O$ of N_2O from surface oceans and terrestrial sources vary widely. We therefore adopt the most depleted, the average, and the most enriched values for these sources in three separate cases [e.g., *Rahn and Wahlen*, 2000; *Perez et al.*, 2000] (see Table 5). To illustrate the importance of stratospheric fractionation on the free troposphere, we compare calculations of the $\delta^{15}N^{bulk}$ and $\delta^{18}O$ isotopic compositions in the free troposphere with stratospheric fractionation and without (i.e., by setting ε = 1.00). The results predict that stratospheric fractionation enriches $\delta^{15}N^{bulk}$ and $\delta^{18}O$ of N_2O in the free troposphere by 5 to 25‰ and 1 to 17‰, respectively, depending on the source isotopic compositions (Note that too little information on the site-specific $\delta^{15}N^{\alpha}$ isotopic compositions of various sources is currently available to make a preliminary estimate, but, on the basis of the large value for $\varepsilon_{app}(^{15}N^{\alpha})$, stratospheric fractionation should have an even larger influence on the free troposphere than for the other isotopologues, as pointed out by *Röckmann et al.* [2003a]). These large ranges are not due to the stratospheric uncertainties but, rather, due to the large uncertainties in the magnitudes and isotopic compositions of the different biogenic sources. As progress is made in characterizing the isotopic composition of the integrated and individual sources [e.g., *Röckmann et al.*, 2003a; *Perez et al.*, 2000], refinements in the stratospheric N_2O loss rate and

Table 4. Net Fluxes of N_2O Isotopologues From the Stratosphere

	ER-2 Observations		3-D Model[a]	
	$\lvert\varepsilon\rvert$ for $N_2O > 200$ ppbv,‰	Net Isotope Flux[b] From $-\varepsilon\cdot$ L, ‰ Tg N yr^{-1}	$\lvert\varepsilon\rvert$, ‰	Net Isotope Flux From $-\varepsilon\cdot$ L, ‰ Tg N yr^{-1}
$^{15}N^{bulk}$	14.9 (±0.5)	192 (±48)	15.0 (±3.0)	196 (±39)
$^{15}N^{\alpha}$	22.5 (±1.2)	290 (±74)	-	-
^{18}O	13.3 (±0.5)	172 (±43)	13.9 (±2.8)	182 (±37)

[a]Table 3b of *McLinden et al.* [2003]; L = 13.1 Tg N yr^{-1} in their model.
[b]L = 13 Tg N yr^{-1}.

Table 5. Box Model Results Estimating the Influence of Stratospheric Fractionation on N_2O Isotopic Compositions in the Free Troposphere

$\delta^{15}N^{bulk}$ of Source N_2O, ‰		$\delta^{15}N^{bulk}$ of Tropospheric N_2O, ‰ Versus Air-N_2		
Soil[a,b]	Ocean[a,c]	At Steady State[d]	No Stratospheric Fractionation[d]	With Stratospheric Fractionation[d]
−34	+2	4.0 [6.1]	−21.2 [−21.3]	+25.2 [27.4]
−14.5	+5	7.1 [6.9]	−7.5 [−7.6]	+14.6 [14.5]
+2	+10	9.9 [7.7]	4.8 [4.7]	+5.1 [3.0]
$\delta^{18}O$ of Source N_2O, ‰		$\delta^{18}O$ of Tropospheric N_2O, ‰ Versus Air-O_2		
Soil	Ocean	At Steady State	No Stratospheric Fractionation	With Stratospheric Fractionation
−4	+14	19.7 [20.3]	2.6 [2.5]	+17.1 [17.8]
+10.5	+14	21.8 [20.9]	12.0 [11.9]	+9.8 [9.0]
+18	+32	24.2 [21.6]	22.7 [22.6]	+1.5 [−1.0]

[a] *Kim and Craig* [1993].
[b] *Perez et al.* [2000].
[c] *Naqvi et al.* [1998].
[d] Calculated assuming stratosphere-troposphere mass exchange across the 100-hPa surface [*Holton*, 1990] (first item in each entry) or the 380 K surface [*Appenzeller et al.*, 1996] (second item, in brackets).

mass flux of air to the troposphere will eventually be required. In the near future, however, now that the fluxes of isotopically enriched N_2O from the stratosphere to the troposphere are quantified to ±25%, additional characterizations of the isotopic composition of individual N_2O sources are needed to further our understanding of the N_2O isotope and concentration budgets.

6. Summary

[56] The $\delta^{15}N^{bulk}$, $\delta^{15}N^{\alpha}$, and $\delta^{18}O$ isotopic compositions of stratospheric N_2O measured on stratospheric whole air samples collected from the NASA ER-2 aircraft during the POLARIS and SOLVE campaigns show that the isotope:N_2O mixing ratio relationships for $N_2O > 200$ ppbv vary little with year, season and latitude. Significant variations in the isotope:N_2O mixing ratio correlations for $N_2O < 200$ ppbv for the ER-2 data are explained by different mixing histories through analyses of simultaneous measurements of the CH_4:N_2O relationships in comparison with satellite observations. From this analysis, we note that a balloon profile of N_2O isotope measurements in the extratropics just prior to the formation of the Arctic vortex would potentially allow a more quantitative analysis of the ER-2 data to be performed exploring the type of mixing that occurs across the vortex edge (e.g., an investigation of late end-member mixing versus continuous weak mixing). An analysis of the ratios of enrichment factors for the ER-2 data shows that the ratios are the same at high and low N_2O mixing ratios to within at least their 2σ uncertainties. Therefore the addition of the ER-2 data to the stratospheric database does not confirm a detectable isotopic signature of a larger contribution of $O(^1D)$ to the total N_2O sink in the lower stratosphere in the ratio $\varepsilon(^{15}N^{\alpha})/\varepsilon(^{15}N^{\beta})$. Additional observations, particularly observations in the deep tropics, would be helpful in resolving whether the difference observed in the balloon data set of *Röckmann et al.* [2001] as analyzed by *Kaiser* [2002] for $N_2O > 179$ ppbv is real and/or due to sample collection in subtropical air and, if so, whether the difference may be due to $O(^1D)$ chemistry or second-order transport and mixing effects. Finally, from the robust isotopologue:N_2O relationships in the lower stratosphere for $N_2O > 200$ ppbv and independent knowledge of the N_2O loss rate, net isotope fluxes of isotopically enriched N_2O due to stratospheric photochemistry were calculated. These fluxes agree to better than the uncertainty in the N_2O loss rate with those calculated with a 3-D chemical-transport model by *McLinden et al.* [2003]. Thus the net stratospheric fluxes should be considered well quantified compared to the remaining uncertainties in the isotopic compositions and magnitudes of the terrestrial and ocean N_2O sources, in agreement with recent analyses by *Röckmann et al.* [2003a] and *Blake et al.* [2003]. Progress in balancing the global N_2O isotope budget will therefore come in the near future from more extensive observations of the isotopic compositions of the various N_2O sources and additional characterization of the underlying biological fractionation mechanisms.

Appendix A: Net Isotope Flux Calculations and Comparisons

[57] Calculating the net isotope flux from the stratosphere where photochemical processes result in isotopic changes in atmospheric N_2O is addressed with a box model by adapting the procedure for $\delta^{13}C$ of atmospheric CO_2 from *Tans et al.* [1993] (see also *Röckmann et al.* [2003a] for box model equations specifically addressing the isotopic change in N_2O sources since the Industrial Revolution). First, the atmospheric mass balance for N_2O is given by equation (A1)

$$\frac{dN}{dt} = T + O + A - L = P - L \equiv \frac{dN_T}{dt} + \frac{dN_S}{dt} = (-F_{TS} + F_{ST} + P) + (F_{TS} - F_{ST} - L) \quad \text{(A1)}$$

where N is the total number of $^{14}N^{14}N^{16}O$ molecules, T and O are terrestrial and oceanic N_2O production rates, A is the average anthropogenic contribution to the N_2O production rate, P is the sum of T, O and A for simplicity (and could include an additional term for the minor atmospheric sources from NH_3 oxidation and $N_2 + O(^1D)$ amounting to 1–2% of the total [*Prather and Ehhalt*, 2001; *Estupiñán et al.*, 2002]) and L is the global loss rate. Separate mass balances for N_2O molecules in the troposphere (N_T) and stratosphere (N_S) can also be expressed and represented by N_2O fluxes between the troposphere and stratosphere (i.e.,

F_{TS} and F_{ST}) along with the production rate, P, and loss rate, L. An equation analogous to equation (A1) can be written for the ^{15}N or ^{18}O of N_2O isotopologues. Instead, however, we can also express the isotopic mass balance in terms of isotope ratios (i.e., $^{15}R = {}^{15}N/N$) characteristic of the N_2O production and loss processes in the troposphere and stratosphere (equation (A2)).

$$\frac{d^{15}N}{dt} = {}^{15}R_P\,P - {}^{15}R_L\,L \equiv \frac{d^{15}N_T}{dt} + \frac{d^{15}N_S}{dt} = \frac{d({}^{15}R_TN_T)}{dt} + \frac{d({}^{15}R_SN_S)}{dt} \quad (A2)$$

Applying the calculus product rule to equation (A2), simplifying it by substituting $dN_T/dt = -F_{TS} + F_{ST} + P$ and $dN_S/dt = F_{TS} - F_{ST} - L$ and then converting the isotope ratio terms to the corresponding delta values using $\delta_i = (R_i/R_{STD} - 1)1000$ and dividing all terms by R_{STD} (where R_{STD} is the isotope ratio for air-N_2 and VSMOW for ^{15}N and ^{18}O), we obtain

$$(\delta_P - \delta_T)P - (\delta_L - \delta_T)L = N_T\frac{d\delta_T}{dt} + N_S\frac{d\delta_S}{dt} + (\delta_S - \delta_T)\frac{dN_S}{dt} \quad (A3)$$

Rather than carry all terms in equation (A3), for our application we can make several simplifying assumptions. First, we can assume that $d\delta_S/dt$ is zero, i.e., that the characteristic fractionation occurring in the stratospheric reservoir is not changing with time. Second, we can assume that dNs/dt, the growth rate of N_2O in the stratosphere, is simply proportional to the growth rate in the troposphere, leading to a value for dNs/dt of $\sim$0.3 Tg N yr^{-1} [e.g., *McElroy and Jones*, 1996]. However, it will become clear in later equations that this value is small compared to the global loss rate of N_2O of 13 Tg N yr^{-1} and including it or not makes only a small difference (up to 2%) in the calculated net isotope fluxes. Thus, in the following equations, the term with factor dNs/dt is also ignored. We note that *Röckmann et al.* [2003a] also assumed that $d\delta_S/dt$ and dNs/dt both equal zero in writing their equation (1).

[58] The remaining terms can be grouped as in equation (A4). In this equation, the term $-(\delta_L - \delta_T)L$

$$-(\delta_L - \delta_T)L = N_T\frac{d\delta_T}{dt} - (\delta_P - \delta_T)P \quad (A4)$$

represents the net isotopic change in the troposphere due to fractionation in the stratospheric loss processes. In other words, it is the net isotope flux from the stratosphere and is usually expressed in ‰ Tg N yr^{-1} or ‰ mol N_2O yr^{-1}. However, a single δ_L for the entire stratosphere cannot easily be determined from the observations. Thus we need to express the net isotope flux with observable quantities. Since $dN_T/dt = -F_{TS} + F_{ST} + P$, $d^{15}N_T/dt = d({}^{15}R_TN_T)/dt \equiv -{}^{15}R_TF_{TS} + {}^{15}R_SF_{ST} + {}^{15}R_PP$, and therefore $N_T \cdot d\delta_T/dt = (\delta_S - \delta_T)F_{ST} + (\delta_p - \delta_T)P$, equation (A4) can therefore be written as

$$-(\delta_L - \delta_T)L = (\delta_S - \delta_T)F_{ST} \quad (A5)$$

Thus the net isotope flux from the stratosphere, $-(\delta_L - \delta_T)L$, is given by the product of the flux of N_2O from the stratosphere to the troposphere and the difference between the isotopic composition of N_2O in air returning to the troposphere and that for N_2O in the free troposphere.

[59] There are now several ways to calculate the net isotope flux given by $(\delta_S - \delta_T)F_{ST}$. First, on the basis of the observed isotope:N_2O relationships in the stratosphere, $(\delta_S - \delta_T)$ can be expressed as

$$\delta_S - \delta_T = (\delta_T + 1000)\cdot((m_S/m_T)^{\varepsilon} - 1) \quad (A6)$$

The loss rate, L, of N_2O is given by equation (A7) (given our assumption noted earlier that dNs/dt = 0):

$$L = F_{TS} - F_{ST} = F(m_T - m_S),\ \text{so that}\ m_S = m_T - L/F \quad (A7)$$

where F is the mass flux of air between the troposphere and stratosphere and m_T and m_S are the mixing ratios of N_2O in the troposphere and stratosphere, respectively. The net isotope flux, $F_{ST}(\delta_S - \delta_T)$, is given by equation (A8)

$$F_{ST}(\delta_S - \delta_T) = (Fm_T - L)\cdot(\delta_T + 1000)\cdot\left(\left(1 - \frac{L}{Fm_T}\right)^{\varepsilon} - 1\right) \quad (A8)$$

and is thus determined by the mass flux of air between the troposphere and stratosphere, F, the N_2O mixing ratio in the troposphere, m_T, the tropospheric N_2O isotopic composition, δ_T, the apparent enrichment factor, ε, and the loss rate of N_2O in the stratosphere, L.

[60] Apart from the assumptions noted after equation (A3), equation (A8) can be considered the most robust way to calculate a net isotope flux for N_2O isotopologues. For comparison among different approaches to estimating the net isotope fluxes that appear in the literature, however, we can make some additional approximations. First, since δ_S for air returning to the troposphere will not be larger than δ_T by $\sim$6‰ in our estimates, the inherent approximation of the Rayleigh relationship expressed in δ values, $\delta_S - \delta_T \cong \varepsilon \cdot \ln(m_S/m_T)$, can also be used in the expression for the net isotope flux (equation (A9)) with an error of only 0.04 to 0.08‰ in δ_S for the N_2O range of interest, relative to those from equation (A6). Thus the net isotope flux, $F_{ST}(\delta_S - \delta_T)$, can be expressed as in equation (A9).

$$F_{ST}(\delta_S - \delta_T) \cong \varepsilon\cdot(F\cdot m_T - L)\cdot\ln(1 - L/Fm_T) \quad (A9)$$

This approximation introduces errors of only 0.2 to 0.3%, 1.2 to 1.4%, and 0.1 to 0.2% in the net isotope fluxes for $^{15}N^{bulk}$, $^{15}N^{\alpha}$, and ^{18}O for the two mass fluxes of *Holton* [1990] and *Appenzeller et al.* [1996], respectively, relative to those derived from equation (A8).

[61] Note, however, that the mass flux of air between the stratosphere and troposphere, F, does not cancel out in these expressions for the net isotope flux. Yet F is not yet well determined and depends on how the tropopause is defined, as noted in main text. However, using the two different mass fluxes of *Holton* [1990] of 2.0×10^{17} kg yr^{-1} and *Appenzeller et al.* [1996] of 6.8×10^{17} kg yr^{-1} in equation (A9) results in differences in the net isotope fluxes of only 8% (see Table 3), a small difference considering the factor of 3 difference in the mass fluxes of air. This small difference is because both δ_S and F_{ST} depend on F: the

larger mass flux yields a higher mixing ratio for N_2O in air returning to the troposphere, which, in turn yields a smaller value for δ_S for N_2O in air returning to the troposphere, as pointed out earlier by *Luz et al.* [1999] and *Röckmann et al.* [2003a].

[62] Some additional approximations can be made to remove the dependence of equation (A9) on F. The natural logarithm term in equation (A9) can be expanded in a Taylor series and truncated as

$$F_{ST}(\delta_S - \delta_T) = \varepsilon \cdot (F \cdot m_T - L) \cdot \ln\left(1 - \frac{L}{F \cdot m_T}\right)$$
$$\approx \varepsilon \cdot (F \cdot m_T - L) \cdot \left(\frac{(1 - L/F \cdot m_T) - 1}{(1 - L/F \cdot m_T)}\right) \approx -\varepsilon \cdot L$$

so that

$$F_{ST}(\delta_S - \delta_T) \approx -\varepsilon \cdot L \quad \text{(A10)}$$

Thus the net isotope flux is approximately equivalent to the product of the apparent enrichment factor, ε, and the N_2O loss rate. This approximate expression yields errors of 3% (12%), 2% (11%), and 1% (8%) in the net isotope fluxes calculated for $^{15}N^{bulk}$, $^{15}N^{\alpha}$, and ^{18}O for the *Holton* [1990] (*Appenzeller et al.* [1996]) mass flux, respectively, relative to those derived from equation (A8). The expression in equation (A10) is what *McLinden et al.* [2003] used to estimate the net isotope fluxes of N_2O isotopologues from their 3-D chemical-transport model.

[63] In addition to the methods above using a Rayleigh fractionation approach with known ε_{app} values, the net isotope flux can also be derived phenomenologically by considering the N_2O isotopologues as long-lived tracers in a *Plumb and Ko* [1992] approach. As noted in the main text, the slope of the correlation between long-lived tracers is equal to their net vertical fluxes. While exact equations expressing the net isotope flux for an isotopologue of N_2O over the net vertical flux of N_2O can be derived from expressions given in equations above, an expression for ε_{app} is still needed. To avoid this, we use a more phenomenological and approximate approach but one that is useful for calculating a net isotope flux in the case that ε_{app} is not well determined because of, for example, multiple fractionation processes involved such as for the ^{17}O–^{18}O isotope anomaly in the stratospheric CO_2 [e.g., *Luz et al.*, 1999]. The slope, μ, of the N_2O isotopic composition: N_2O mixing ratio relationship, which is linear in the lower stratosphere for $N_2O > 200$ ppbv, can be written as

$$\mu = \frac{\delta_S - \delta_T}{m_S - m_T} \quad \text{(A11)}$$

Substituting equation (A11) for $\delta_S - \delta_T$, the net isotope flux can be expressed as

$$F_{ST}(\delta_S - \delta_T) \approx Fm_S \cdot \mu \cdot (m_S - m_T) = -\mu \cdot m_S \cdot L$$
$$= -\mu \cdot (m_T - L/F) \cdot L \quad \text{(A12)}$$

Note that this expression also depends on the mass flux of air, F. The differences in the net isotope fluxes between equation (A12) and equation (A8) are 9% (19%), 10% (20%), and 9% (19%) for $^{15}N^{bulk}$, $^{15}N^{\alpha}$, and ^{18}O, respectively, for the air mass flux of *Holton* [1990] (of *Appenzeller et al.* [1996]). Thus the equations based on observed ε_{app} values are clearly the preferable approach for N_2O, for which a well-defined ε_{app} is known.

[64] Overall, to within the approximations stated, the box model approach and the *Plumb and Ko* [1992] approach are essentially equivalent, depend on the mass flux of air between the stratosphere and troposphere but to less than the current uncertainty in L, and can be largely approximated by simply multiplying the enrichment factors by the N_2O loss rate, as *McLinden et al.* [2003] have done. This analysis also shows that the concerns of *Rahn and Wahlen* [2000] over uncertainties in the mass flux of air and in the effects of transport on the enrichment factors do not result in overall uncertainties in the isotope fluxes significantly larger than current uncertainty in the N_2O global loss rate.

[65] **Acknowledgments.** We thank Stephen Donnelly, Rich Lueb, Sue Schauffler, and Verity Stroud for support of the ER-2 whole air sampling and methane measurements; Michael Bender for valuable guidance and advice as well as measurements of $\delta^{15}N$ of N_2; Jan Kaiser, Thomas Röckmann, and Carl Brenninkmeijer for advice on measurements of site-specific $\delta^{15}N$ of N_2O and some helpful comments on the manuscript during review; and M. Loewenstein, H. Jost, and J. Podolske for in situ measurements of N_2O during the POLARIS campaign. This work was supported by grants to UC Berkeley from the National Science Foundation Atmospheric Chemistry Program (ATM-9901463), the NASA Upper Atmospheric Research Program (NAG2-1483), and the David and Lucile Packard Foundation and by grants to NCAR from the NASA Upper Atmospheric Research Program and the National Science Foundation. The National Center for Atmospheric Research is operated by the University Corporation for Atmospheric Research under the sponsorship of the National Science Foundation.

References

Andrews, A. E., K. A. Boering, B. C. Daube, S. C. Wofsy, E. J. Hintsa, E. M. Weinstock, and T. P. Bui (1999), Empirical age spectra for the lower tropical stratosphere from in situ observations of CO_2, Implications for stratospheric transport, *J. Geophys. Res.*, *104*(D21), 26,581–26,595.

Andrews, A. E., et al. (2001), Mean ages of stratospheric air derived from in situ observations of CO_2, CH_4, and N_2O, *J. Geophys. Res.*, *106*(D23), 32,295–32,314.

Appenzeller, C., J. R. Holton, and K. H. Rosenlof (1996), Seasonal variation of mass transport across the tropopause, *J. Geophys. Res.*, *101*(D10), 15,071–15,078.

Begun, G. M., and L. Landau (1961), Mass spectra and metastable transitions in isotopic nitrous oxides, *J. Chem. Phys.*, *35*(2), 547–551.

Blake, G. A., M.-C. Liang, C. G. Morgan, and Y. L. Yung (2003), A Born-Oppenheimer photolysis model and its application to N_2O isotopic fractionation, *Geophys. Res. Lett.*, *30*(12), 1656, doi:10.1029/2003GL016932.

Bouwman, A. F., K.W. Van der Hoek, and J. G. J. Oliver (1995), Uncertainties in the global source distribution of nitrous oxide, *J. Geophys. Res.*, *100*(D2), 2785–2800.

Brand, W. A. (1995), Precon: A fully automated interface for the Pre-GC concentration of trace gases in air for isotopic analysis, *Isot. Environ. Health Stud.*, *31*, 277–284.

Brasseur, G., and S. Solomon (1986), *Aeronomy of the Middle Atmosphere*, 2nd ed., D. Reidel, Norwell, Mass.

Brenninkmeijer, C. A. M., and T. Röckmann (1999), Mass spectrometry of the intramolecular nitrogen isotope distribution of environmental nitrous oxide using fragment-ion analysis, *Rapid Commun. Mass. Spectrom.*, *13*, 2028–2033.

Criss, R. E. (1999), *Principles of Stable Isotope Distribution*, pp. 21–23, Oxford Univ. Press, New York.

Estupiñán, E. G., J. M. Nicovich, J. Li, D. M. Cunnold, and P. H. Wine (2002), Investigation of N_2O production from 266 and 532 nm laser flash photolysis of $O_3/N_2/O_2$ mixtures, *J. Phys. Chem. A*, *106*(24), 5880–5890.

Flocke, F., et al. (1999), An examination of chemistry and transport processes in the tropical lower stratosphere using observations of long-lived and short-lived compounds obtained during STRAT and POLARIS, *J. Geophys. Res.*, *104*(D21), 26,625–26,642.

Griffith, D. W., G. C. Toon, B. Sen, J. F. Blavier, and R. A. Toth (2000), Vertical profiles of nitrous oxide isotopomer fractionation measured in the stratosphere, *Geophys. Res. Lett.*, *27*(16), 2485–2488.

Herman, R. L., et al. (1998), Tropical entrainment time scales inferred from stratospheric N_2O and CH_4 observations, *Geophys. Res. Lett.*, *25*(15), 2781–2784.

Holton, J. R. (1990), On the global exchange of mass between the stratosphere and troposphere, *J. Atmos. Sci.*, *47*(3), 392–395.

Hurst, D. F., et al. (2000), Comparison of in situ N_2O and CH_4 measurements in the upper troposphere and lower stratosphere during STRAT and POLARIS, *J. Geophys. Res.*, *105*(D15), 19,811–19,822.

Hurst, D. F., et al. (2002), Construction of a unified, high-resolution nitrous oxide data set for ER-2 flights during SOLVE, *J. Geophys. Res.*, *107*(D20), 8271, doi:10.1029/2001JD000417.

Johnson, M. S., G. D. Billing, A. Groudis, and H. M. Janssen (2001), Photolysis of nitrous oxide isotopomers studied by time-dependent Hermite propagation, *J. Phys. Chem. A*, *105*, 8672–8680.

Johnston, J. C., S. S. Cliff, and M. H. Thiemens (1995), Measurement of multioxygen isotopic ($\delta^{18}O$ and $\delta^{17}O$) fractionation factors in the stratospheric sink reactions of nitrous oxide, *J. Geophys. Res.*, *100*(D8), 16,801–16,804.

Jost, H., M. Loewenstein, L. Pfister, J. J. Margitan, A. Y. Chang, and R. J. Salawitch (1998), Laminae in the tropical middle stratosphere: Origin and age estimation, *Geophys. Res. Lett.*, *25*(23), 4337–4340.

Kaiser, J. (2002), Stable isotope investigations of atmospheric nitrous oxide, Ph.D. dissertation, Johannes Gutenberg Univ., Mainz, Germany.

Kaiser, J., T. Röckmann, and C. A. M. Brenninkmeijer (2002a), Intramolecular ^{15}N and ^{18}O fractionation in the reaction of N_2O with O (^1D) and its implications for the stratospheric N_2O isotope signature, *J. Geophys. Res.*, *107*(D14), 4214, doi:10.1029/2001JD001506.

Kaiser, J., T. Röckmann, and C. A. M. Brenninkmeijer (2002b), Temperature dependence of isotope fractionation in N_2O photolysis, *Phys. Chem. Chem. Phys.*, *4*, 4420–4430.

Kaiser, J., T. Röckmann, C. A. M. Brenninkmeijer, and P. J. Crutzen (2003a), Wavelength dependence of isotope fractionation in N_2O photolysis, *Atmos. Chem. Phys.*, *3*, 303–315.

Kaiser, J., S. Park, K. A. Boering, C. A. M. Brenninkmeijer, A. Hilkert, and T. Röckmann (2003b), Mass-spectrometric method for the absolute calibration of the intramolecular nitrogen isotope distribution in nitrous oxide, *Anal. Bioanal. Chem.*, doi:10.1007/s00216-003-2233-2, in press.

Kim, K.-R., and H. Craig (1993), Nitrogen-15 and oxygen-18 characteristics of nitrous oxide: A global perspective, *Science*, *262*, 1855–1857.

Kondo, Y., et al. (1999), NO_y-N_2O correlation observed inside the Arctic vortex in February 1997: Dynamical and chemical effects, *J. Geophys. Res.*, *104*(D7), 8215–8224.

Kroeze, C., A. Mosier, and L. Bouwman (1999), Closing the global N_2O budget: A retrospective analysis 1500–1994, *Global Biogeochem. Cycles*, *13*(1), 1–8.

Luz, B., E. Barkan, M. L. Bender, M. H. Thiemens, and K. A. Boering (1999), Triple-isotope composition of atmospheric oxygen as a tracer of biosphere productivity, *Nature*, *400*, 547–550.

McCarthy, M. C., K. A. Boering, A. L. Rice, S. C. Tyler, P. Connell, and E. Atlas (2003), Carbon and hydrogen isotopic compositions of stratospheric methane: 2. Two-dimensional model results and implications for kinetic isotope effects, *J. Geophys. Res.*, *108*(D15), 4461, doi:10.1029/2002JD003183.

McElroy, M. B., and D. B. A. Jones (1996), Evidence for an additional source of atmospheric N_2O, *Global Biogeochem. Cycles*, *10*(4), 651–659.

McLinden, C. A., S. C. Olsen, B. Hannegan, O. Wild, and M. J. Prather (2000), Stratospheric ozone in 3-D models: A simple chemistry and the cross-tropopause flux, *J. Geophys. Res.*, *105*(D11), 14,653–14,665.

McLinden, C. A., M. J. Prather, and M. S. Johnson (2003), Global modeling of N_2O isotopomers: Stratospheric enrichment, iso-budgets and the ^{17}O–^{18}O mass-independent anomaly, *J. Geophys. Res.*, *108*(D8), 4233, doi:10.1029/2002JD002560.

Merritt, D. A., and J. M. Hayes (1994), Nitrogen isotopic analyses by isotope-ratio-monitoring gas chromatography/mass spectrometry, *J. Am. Soc. Mass Spectrom.*, *5*, 387–397.

Michelsen, H. A., G. L. Manney, M. R. Gunson, and R. Zander (1998), Correlations of stratospheric abundances of CH_4 and N_2O derived from ATMOS measurements, *Geophys. Res. Lett.*, *25*(15), 2777–2780.

Michelsen, H. A., et al. (1999), Intercomparison of ATMOS, SAGE II, and ER-2 observations in Arctic vortex and extra-vortex air masses during spring 1993, *Geophys. Res. Lett.*, *26*(3), 291–294.

Miller, J. B., and P. P. Tans (2003), Calculation of isotopic fractionation from atmospheric measurements at various scales, *Tellus, Ser. B*, *55*, 207–214.

Minschwaner, K., R. J. Salawitch, and M. B. McElroy (1993), Absorption of solar radiation by O_2: Implications for O_3 and lifetimes of N_2O, CFC_{13}, and CF_2Cl_2, *J. Geophys. Res.*, *98*(D6), 10,543–10,561.

Morgan, C. G., M. Allen, M. C. Liang, R. L. Shia, G. A. Blake, and Y. L. Yung (2003), Isotopic fractionation of nitrous oxide in the stratosphere: Comparison between model and observations, *J. Geophys. Res.*, *108*, doi:10.1029/2003JD003402, in press.

Mosier, A., C. Kroeze, C. Nevison, O. Oenema, S. Seitzinger, and O. van Cleemput (1998), Closing the global N_2O budget: Nitrous oxide emissions through the agricultural nitrogen cycle, *Nutrient Cycling Agroecosyst.*, *52*, 225–248.

Murphy, D. M., and D. W. Fahey (1994), An estimate of the flux of stratospheric reactive nitrogen and ozone into the troposphere, *J. Geophys. Res.*, *99*(D3), 5325–5332.

Murphy, D. M., D. W. Fahey, M. H. Proffitt, S. C. Liu, K. R. Chan, C. S. Eubank, S. R. Kawa, and K. K. Kelly (1993), Reactive nitrogen and its correlation with ozone in the lower stratosphere and troposphere, *J. Geophys. Res.*, *98*(D5), 8751–8773.

Naqvi, A. S. W., T. Yoshinari, D. A. Jayakumar, M. A. Altabet, P. V. Narvekar, A. H. Devol, J. A. Brandes, and L. A. Codispoti (1998), Budgetary and biogeochemical implications of N_2O isotope signatures in the Arabian Sea, *Nature*, *394*, 462–464.

Newman, P. A., D. W. Fahey, W. H. Brune, and M. J. Kurylo (1999), Preface to Photochemistry of Ozone Loss in the Arctic Region in Summer (POLARIS) special issue, *J. Geophys. Res.*, *104*(D21), 26,481–26,495.

Newman, P. A., et al. (2002), An overview of the SOLVE/THESEO 2000 campaign, *J. Geophys. Res.*, *107*(D20), 8259, doi:10.1029/2001JD001303.

Olsen, S. C., C. A. McLinden, and M. J. Prather (2001), Stratospheric N_2O-NOy system: Testing uncertainties in a three-dimensional framework, *J. Geophys. Res.*, *106*(D23), 28,771–28,784.

Park, S., E. Atlas, and K. A. Boering (2002), Observations of the fractionation of nitrous oxi'de isotopomers in the stratosphere, *Eos Trans. AGU*, *83*(19), Spring Meeting Suppl., S94.

Perez, T. S., S. C. Trumbore, S. C. Tyler, P. A. Matson, I. Ortiz-Monasterio, T. Rahn, and D. W. T. Griffith (2000), Isotopic variability of N_2O emissions from tropical forest soils, *Global Biogeochem. Cycles*, *14*(2), 525–535.

Plumb, R. A., and M. K. W. Ko (1992), Interrelationships between mixing ratios of long-lived stratospheric constituents, *J. Geophys. Res.*, *97*(D9), 10,145–10,156.

Plumb, R. A., D. W. Waugh, and M. P. Chipperfield (2000), The effects of mixing on tracer relationships in the polar vortices, *J. Geophys. Res.*, *105*(D8), 10,047–10,062.

Podolske, J. R., and M. Loewenstein (1993), Airborne tunable diode laser spectrometer for trace-gas measurements in the lower stratosphere, *Appl. Opt.*, *32*, 5324–5333.

Prather, M., and D. Ehhalt (2001), Atmospheric chemistry and greenhouse gases, in *Climate Change 2001: The Scientific Basis, Contribution of Working Group I to the Third Assessment Report of the Intergovernmental Panel on Climate Change*, edited by J. T. Houghton et al., pp. 239–287, Cambridge Univ. Press, New York.

Rahn, T., and M. Wahlen (1997), Stable isotope enrichment in stratospheric nitrous oxide, *Science*, *278*, 1776–1778.

Rahn, T., and M. Wahlen (2000), A reassessment of the global isotopic budget of atmospheric nitrous oxide, *Global Biogeochem. Cycles*, *14*(2), 537–543.

Rahn, T., H. Zang, M. Wahlen, and G. A. Blake (1998), Stable isotope fractionation during ultraviolet photolysis of N_2O, *Geophys. Res. Lett.*, *25*(24), 4489–4492.

Rahn, T., J. M. Eiler, K. A. Boering, P. O. Wennberg, M. C. McCarthy, S. Tyler, S. Schauffler, S. Donnelly, and E. Atlas (2003), Extreme deuterium enrichment in stratospheric molecular hydrogen and its significance for the global atmospheric budget of H_2, *Nature*, *424*, 918–921.

Rex, M., et al. (1999), Subsidence, mixing, and denitrification of Arctic polar vortex air measured during POLARIS, *J. Geophys. Res.*, *104*(D21), 26,611–26,623.

Rice, A. L., S. C. Tyler, M. C. McCarthy, K. A. Boering, and E. Atlas (2003), The carbon and hydrogen isotopic compositions of stratospheric methane: 1. High-precision observations from the NASA ER-2 aircraft, *J. Geophys. Res.*, *108*(D15), 4460, doi:10.1029/2002JD003042.

Ricker, W. E. (1973), Linear regression in fishery research, *J. Fish. Res. Board Can.*, *30*, 409–434.

Röckmann, T., C. A. M. Brenninkmeijer, M. Wollenhaupt, J. N. Crowley, and P. J. Crutzen (2000), Measurement of the isotopic fractionation of $^{15}N^{14}N^{16}O$, $^{14}N^{15}N^{16}O$ and $^{14}N^{14}N^{18}O$ in the UV photolysis of nitrous oxide, *Geophys. Res. Lett.*, *27*(9), 1399–1402.

Röckmann, T., J. Kaiser, and C. A. M. Brenninkmeijer (2001), Isotopic enrichment of nitrous oxide ($^{15}N^{14}NO$, $^{14}N^{15}NO$, $^{14}N^{14}N^{18}O$) in the stratosphere and in the laboratory, *J. Geophys. Res.*, *106*(D10), 10,403–10,410.

Röckmann, T., J. Kaiser, and C. A. M. Brenninkmeijer (2003a), The isotopic fingerprint of the pre-industrial and the anthropogenic N_2O source, *Atmos. Chem. Phys.*, *3*, 315–323.

Röckmann, T., J. Kaiser, C. A. M. Brenninkmeijer, and W. A. Brand (2003b), Gas chromatography/isotope-ratio mass spectrometry method for high-precision position-dependent ^{15}N and ^{18}O measurements of atmospheric nitrous oxide, *Rapid Comm. Mass. Spectrom.*, *17*, 1897–1908.

Tans, P. P., J. A. Berry, and R. F. Keeling (1993), Oceanic C-13/C-12 observations: A new window on ocean CO_2 uptake, *Global Biogeochem. Cycles*, *7*(2), 353–368.

Toyoda, S., and N. Yoshida (1999), Determination of nitrogen isotopomers of nitrous oxide on a modified isotope ratio mass spectrometer, *Anal. Chem.*, *71*, 4711–4718.

Toyoda, S., N. Yoshida, T. Urabe, S. Aoki, T. Nakazawa, S. Sugawara, and H. Honda (2001), Fractionation of N_2O isotopomers in the stratosphere, *J. Geophys. Res.*, *106*(D7), 7515–7522.

Turatti, F., D. W. T. Griffith, S. R. Wilson, M. B. Esler, T. Rahn, H. Zhang, and G. A. Blake (2000), Positionally dependent N-15 fractionation factors in the UV photolysis of N_2O determined by high resolution FTIR spectroscopy, *Geophys. Res. Lett.*, *27*(16), 2489–2492.

Waugh, D. W., et al. (1997), Mixing of polar vortex air into middle latitudes as revealed by tracer-tracer scatterplots, *J. Geophys. Res.*, *102*(D11), 13,119–13,134.

Williamson, J. H. (1968), Least-squares fitting of a straight line, *Can. J. Phys.*, *46*(16), 1845.

Yoshida, N., and S. Matsuo (1983), Nitrous isotope ratio of atmospheric N_2O as a key to the global cycle of N_2O, *Geochem. J.*, *17*, 231–239.

Yoshida, N., and S. Toyoda (2000), Constraining the atmospheric N_2O budget from intramolecular site preference in N_2O isotopomers, *Nature*, *405*, 330–334.

Yung, Y. L., and C. E. Miller (1997), Isotopic fractionation of stratospheric nitrous oxide, *Science*, *278*, 1778–1780.

Zhang, H., P. O. Wennberg, V. H. Wu, and G. A. Blake (2000), Fractionation of $^{14}N^{15}NO$ and $^{15}N^{14}NO$ during photolysis at 213 nm, *Geophys. Res. Lett.*, *27*(16), 2481–2484.

E. L. Atlas, Atmospheric Chemistry Division, National Center for Atmospheric Research, P. O. Box 3000, Boulder, CO 80307, USA. (atlas@acd.ucar.edu)

K. A. Boering and S. Park, Department of Earth and Planetary Science, University of California, Berkeley, Latimer Hall, Berkeley, CA 94720-1460, USA. (boering@cchem.berkeley.edu; sunyoung@uclink.berkeley.edu)